A ROS-Activatable Agent Elicits Homologous Recombination DNA Repair and Synergizes with Pathway Compounds

Article *in* ChemBioChem · September 2015

DOI: 10.1002/cbic.201500304

CITATION
1

READS
240

8 authors, including:

Mark Wunderlich
Cincinnati Children's Hospital Medical Center
71 PUBLICATIONS **1,744** CITATIONS
SEE PROFILE

Michael Wyder
University of Cincinnati
21 PUBLICATIONS **484** CITATIONS
SEE PROFILE

Ana Luisa Kadekaro
University of Cincinnati
35 PUBLICATIONS **1,379** CITATIONS
SEE PROFILE

James C Mulloy
Cincinnati Children's Hospital Medical Center
121 PUBLICATIONS **4,088** CITATIONS
SEE PROFILE

A EUROPEAN JOURNAL OF CHEMICAL BIOLOGY

CHEMBIOCHEM

SYNTHETIC BIOLOGY & BIO-NANOTECHNOLOGY

Accepted Article

Title: A ROS-activatable agent elicits homologous recombination DNA repair and synergizes with pathway compounds

Authors: Fathima Shazna Thowfeik; Safnas F. AbdulSalam; Mark Wunderlich; Michael Wyder; Kenneth D. Greis; Ana L. Kadekaro; James C. Mulloy; Edward Joseph Merino

To be cited as: ChemBioChem 10.1002/cbic.201500304

Link to VoR: http://dx.doi.org/10.1002/cbic.201500304

A Journal of

ChemPubSoc Europe

www.chembiochem.org

WILEY-VCH

FULL PAPER WILEY-VCH

A ROS-activatable agent elicits homologous recombination DNA repair and synergizes with pathway compounds

Fathima Shazna Thowfeik[a], Safnas F. AbdulSalam[a], Mark Wunderlich[b], Michael Wyder[d], Kenneth D. Greis[d], Ana L. Kadekaro[c], James C. Mulloy[b], Edward J. Merino*[a]

Abstract: We have designed ROS-activated cytotoxic agents that are active against AML cancer cells. In this study the mechanism and synergistic effects against cells co-expressing the AML oncogenes MLL-AF9 fusion and FLT3-ITD was investigated. The agent had an IC50 value of 1.8±0.3 μM with a selectivity of 9-fold compared to untransformed cells. Treatment induced DNA strand breaks, apoptosis, and cell cycle arrest. Proteomics and transcriptomics revealed enhanced expression of the pentose phosphate pathway, DNA repair, and pathways common to cell stress. Western blotting confirmed repair by homologous recombination. Importantly, **RAC1** treatment was synergistic in combination with multiple pathway targeting therapies in AML cells but less so in untransformed cells. Taken together, these results demonstrate that **RAC1** can selectively target poor prognosis AML and do so by creating DNA double strand breaks that require homologous recombination.

Introduction

Agents that alter or modify DNA play a central role as anti-cancer agents.[1] The development of these agents has taken a back seat to the development of kinase inhibitors and antibody therapies due to their exquisite selectivity. For example, the success of targeting chronic myelogenous leukemia harboring the unique fusion protein made by a t(9;22)(q34;q11) translocation by gleevac is well known.[2] Interestingly, despite decades of effort, agents that modify, bind, or limit DNA metabolism still hold a coveted position in the treatment of cancers. In acute myeloid leukemia (AML) the standard of care remains daunorubicin, a DNA intercalator, and cytosine arabinoside, a DNA metabolism inhibitor. The reason for the success of DNA alteration is simple. In principle the formation of a single or few alterations or inhibitory events within the three billion base pair genome can be sufficient to cause cancer cell apoptosis due to lack of repair, which represents a reaction yield of 10^{-8}.[3,4] In recent times the development of DNA altering agents has been extended to conjugation with cell-targeting antibodies as in the case of the CD33-targeted antibody in gemtuzumab ozogamicin.[5] We are using an alternative and complementary approach based on selective activation by reactive oxygen species (ROS) to design next generation smart DNA modifiers termed ROS-activated cytotoxic agents (RACs).[6,7] In this manuscript we investigate the role and mechanism of DNA repair in treated cells to better understand the DNA modifying action of these novel RAC agents (Figure 1).

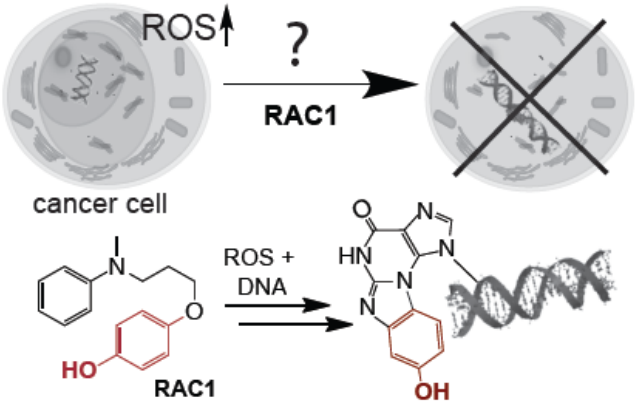

Figure 1. Mechanism of ROS activated cytotoxic agents (RACs). AML is thought to be addicted to elevated levels of ROS, thus we have designed new agents that are activated by ROS and selective to AML. In this manuscript we examine its cellular mechanism. The bottom shows the known chemical reaction **RAC1** undergoes.

Selective activation of a DNA-modifying agent is a means to access the benefits of DNA damage while enhancing agent selectivity. This is a common yet underappreciated strategy in many natural products. Classically, the natural product mitomycin C is selectively activated by reduction into a potent DNA cross-linking agent within cancer cells.[8] More recently the diazo-containing class of natural products, like lomaiviticins and kinamycins, were found to damage DNA in a free radical-mediated activation process.[9] Our designs take advantage of elevated ROS in select cancers. Not every cancer has elevated ROS, but for those that do, ROS-activation represents a powerful means to activate a DNA modifying agent. Current data shows that AML is a cancer with elevated ROS.[10,11] For example, AML cells have high levels of NADPH oxidases that generate superoxide ROS to enhance growth.[12,13] Excessive ROS production is associated with transformation by FLT3 upon internal tandem duplication of the receptor.[14,15] Furthermore, the activity of several AML-associated tyrosine kinases and transcription factors, including Stat5, PI3-kinase, and Src, is altered by ROS.[16-18] The compound under investigation, **RAC1**, has interesting chemical reactivity that led us to further investigate its mechanism of action (Figure 1, bottom). First, oxidation leads to a potent electrophile that a DNA arylamine (guanine, cytosine, adenine) can attack by 1,2-addition followed by Michael addition and elimination to yield an unusual hydroxy-benzethenoguanine adduct. Based on chemical mechanism it is unlikely to be a DNA cross-linker but nevertheless elicits a fifty percent loss of cell viability at 700nM in AML cells. DNA repair is a complex process mediated by multiple different mechanisms. For DNA modifying agents, induction of double strand breaks is a sought after mechanism, since formation of such lesions are highly cytotoxic. In this manuscript we examine the mechanism of cellular cytotoxicity of RACs against AML cells and explore the likely mechanism of DNA repair.

[a] F. S. Thowfeik, S. F. AbdulSalam, Prof. E.J. Merino
Department of Chemistry
University of Cincinnati
404 Crosley Tower, Cincinnati OH. 45221-0172 (USA)
E-mail: merinoed@ucmail.uc.edu
[b] M. Wunderlich, Prof. J. C. Mulloy
Division of Experimental Hematology and Cancer Biology
Cincinnati Children's Hospital Medical Center
Cincinnati, OH 45221
[c] Prof. A. L. Kadekaro
Department of Dermatology
University of Cincinnati College of Medicine
Cincinnati, OH. 45221
[d] M. Wyder, Prof. K. D. Greis
Department of Cancer Biology
University of Cincinnati College of Medicine
Cincinnati, OH. 45221

Supporting information for this article is available on the WWW under ((Please delete this text if not appropriate))

Results and Discussion

A RAC agent shows selective toxicity against a common type of AML

To test the efficacy of the RAC agent, we used primary human CD34+ blood stem cells that were transformed with the MLL-AF9 fusion protein and internal tandem duplication of FLT3 (MLL-AF9 ITD). This transformation represents a good model for poor prognosis AML.[19] **RAC1** showed highly selective cytotoxicity against this transformed cell line with an IC50 value of 1.8±0.3 μM whereas normal CD34+ blood cells showed an IC50 of 16.1±0.5 μM (Figure 2A). We next investigated key markers of oxidative stress between the AML cells and untransformed cells. We first investigated the levels of the key antioxidant protein catalase in these two cell lines. The protein concentration of catalase was chosen for interrogation since data mining in HemaExplorer, a new curated database of mRNA expression in AML and normal cells,[20] showed a strong reduction in catalase mRNA expression in AML cells from patients ($p<0.0001$;Figure 2B) with a median reduction of 29%. Cells were grown to modest density, protein extracted, and relative expression of catalase to β-actin quantified (Figure 2C). It was found that untransformed cells had an expression of 1.0±0.07 while the AML cells had a statistically significant decrease to 0.68±0.09 ($p<0.04$). A key question was to determine if poor prognosis AML displays excessive ROS. Basal ROS level measurement via DCF assay reveled the 2.1± 0.2 ($p<0.0001$) fold high levels of ROS in AML cells compared to untransformed cells (Figure 2D). Next we investigated if ROS led to mutagenic DNA lesions by quantifying 8-oxo-7,8-dihydro-2'-deoxyguanosine via an Elisa assay (Figure 2E). In agreement with our hypothesis the data showed that the untransformed cells had a relative 8-oxo-7,8-dihydro-2'-deoxyguanosine concentration of 1.0±0.03 while the AML cells had a concentration of 1.71±0.04 ($p<0.006$). Not only does transformation lower anti-oxidants but it also enhances DNA oxidation. Thus poor prognosis AML is a viable target for **RAC1** due to its elevated ROS-status.

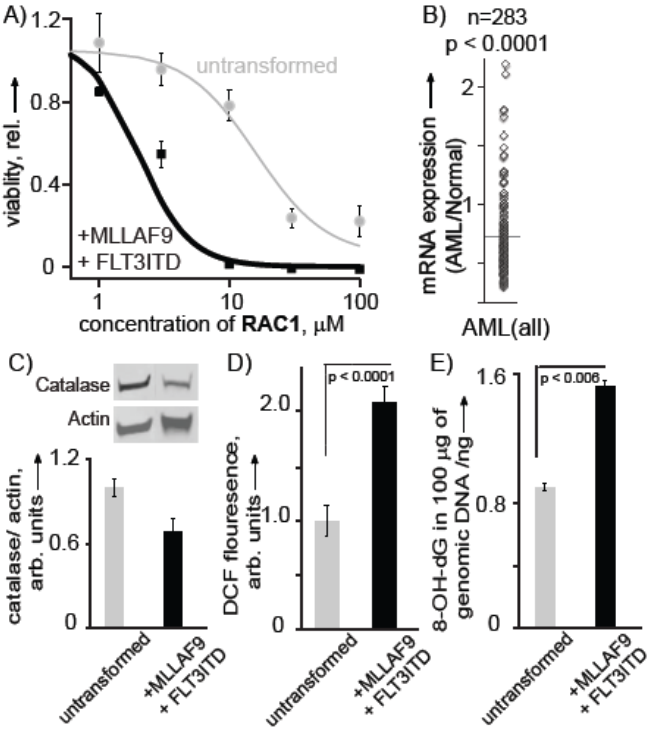

Figure 2. Selective activity of **RAC1**. A) **RAC1** displays highly selective activity against an AML cell line expressing both MLL-AF9 and FLT3-ITD. Viability of AML cells (black) and untransformed blood stem cells (grey) is shown. B) Extracted data from HemeExplorer[20] indicating patient AML samples have reduced catalase antioxidant mRNA. Transformation with MLL-AF9 and FLT3-ITD leads to more oxidative stress as measured by a reduction in the anti-oxidant enzyme catalase via western blot analysis C). Basal ROS levels in AML and untransformed cells measured via DCF assay D) and an increase in 8-oxo-7,8-dihydro-2'-deoxyguanosine measured by Elisa E). Results are presented as means ± SEM from biological triplicates.

Treatment causes DNA strand breaks and apoptosis

Apoptosis is the expected outcome for a reactive cytotoxic agent like **RAC1**. To determine whether cell death by **RAC1** was due to the induction of apoptosis, annexin V/PI staining was assessed. Unstressed cells, treated with vehicle for 48 hours, showed 13.9 ± 0.9 percent of the cells in apoptosis. As a positive control AML cells were irradiated in the UVB region (280-315 nm). Irradiation increased the percent apoptosis to 43.2 ± 0.5 ($p<0.001$). Treatment by **RAC1** led to an increase in the percent apoptosis by 1.2 fold (17.0 ± 0.3%; $p<0.03$) over 24 hours and 2.2 fold (30.8 ± 1.5%; $p<0.001$) at 48 hours (Figure 3A).

Importantly we show direct evidence of cellular DNA damage. DNA damage and repair strand breaks induced by **RAC1** were assessed by single cell gel electrophoresis (comet assay). AML cells were treated at 2 μM for 4 hours and as a positive control cells were irradiated in the UVB region (280-315 nm) (Figure 3B). Untreated cells has 10.0 ± 0.5% DNA in the tail. Irradiation led to an increase to 27.5 ± 1.9% of DNA in the tail ($p<0.0001$). Treatment by **RAC1** led to an increase to 19.5 ± 0.6% DNA in the tail indicating a 2-fold increase ($p<0.0001$). Taken together we conclude that upon failure to repair the DNA damage induced by **RAC1**, cells undergo death via apoptosis.

To investigate cell cycle perturbations by **RAC1,** flow cytometry analysis of BrdU cell cycle assay was performed. The data is shown in Figure 3C. Unstressed cells, treated with vehicle for 24 hours showed 38.7 ± 0.3%, 54.7 ± 1.6% and 6.5 ± 0.2% cells in G0/G1, S phase and G2/M phase respectively. Addition of **RAC1** followed by 12 hours of incubation led to a 27.2 ± 3.1%, 70.0 ± 4.6% and 2.8 ± 0.9% cells in G0/G1, S and G2/M phase respectively with the change in S phase increasing

more than 15% (p-value< 0.001) and a large loss in the AML cells in G2/M. Similar analysis after 24 hours showed 27.0 ± 2.2%, 71.0 ± 3.3% and 1.9 ± 1.2% cells in G0/G1, S and G2/M phase respectively over 24 hours. Thus further confirms that cells are arrested in the S-phase (p-value< 0.001) and cannot reach the G2/M phase. Thus, AML cells try to synthesize damaged DNA (Figure 2C) but fail, leading to strand breaks and apoptosis (Figure 3A and B). This data left important questions regarding the DNA repair mechanism.

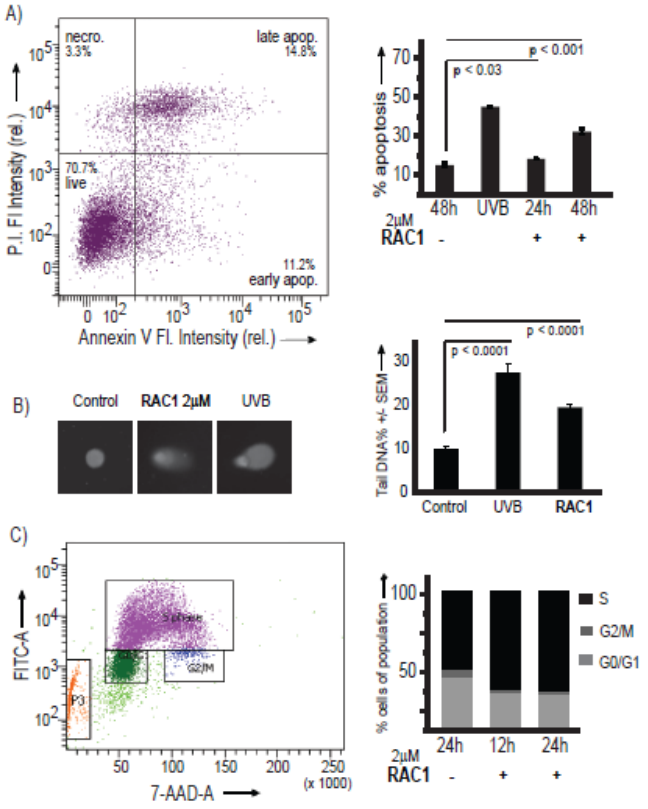

Figure 3. Treatment leads to apoptosis and DNA damage. A) Left. Representative flow cytometer plot. Right. Assessment of percent apoptosis upon treatment with **RAC1** in AML. B) Left. Representative images of AML cells after treatment with **RAC1** and single cell electrophoresis. Right. Quantification of strand breaks upon treatment of **RAC1**. C) Left. Representative cell cycle analysis plot. Right. Assessment of percent cells in each cell cycle phase upon treatment with **RAC1** in AML. Results are presented as means±SEM from biological triplicates.

High-throughput methods to elucidate cellular responses

In order to assess the mechanism of action of **RAC1** in an unbiased manner a quantitative proteomics approach was used. Since the data in Figure 3 showed elevated damage to genomic DNA as a consequence of **RAC1**, the proteomics analysis was targeted to isolated nuclei. This has the added advantage of enriching DNA damage response proteins that are generally low in concentration and/or activated by post-translational modification thereby providing the best opportunity to detect differences in these proteins between controls and treatments. The supporting information (Figure S1, Table S1) shows that nuclear isolation enriched the nuclear marker, lamin A, by 9-fold. We choose the 24 hour time point for analysis since expression changes, rather than post-translational modification, occur on this time-scale. Interestingly because of these criteria we were able to elucidate key protein pathway changes.

Nuclear proteins extracted from AML cells after treatment with **RAC1** or vehicle control were separated by 2-D gel electrophoresis from pI 3-10 and in the 10-300 kD range. Image analysis revealed that 12 proteins (p<0.05) changed in concentration in response to treatment, with 10 proteins increasing, 2 decreasing. Supplementary figure (Figure S2) shows the example of the 2D gel image and an example of a protein spot that increased in concentration after **RAC1** treatment (circled). Of the twelve differentially expressed proteins, eleven were successfully identified by MALDI-TOF/TOF and MS/MS analysis. The characteristics of all identified proteins, including protein name, NCBI accession number, fold change and ANOVA p-value are all summarized in Table 1.

Significantly regulated proteins can be categorized into two groups, proteins involved in DNA damage repair and proteins involved in cancer cell survival mechanisms/ROS homeostasis. Among the proteins that increased upon treatment, transitional endoplasmic reticulum ATPase (VCP/p97) showed the highest fold change of 3.4 (p<0.003). The protein VCP/p97 activates the nuclear factor-kB signaling pathway and has recently been under intense study.[21-25] Functionally, VCP/p97 remodels multimeric protein complexes that have multiple ubiquitins, like nucleosome core particles, to initiate DNA repair. VCP/p97 is essential to double strand break repair in an RNF8 and ubiquitin-dependent manner, where it facilitates the recruitment of BRCA1 and the tumor suppressor 53BP1 to DNA lesions. VCP/97 has also been associated in repair by both non-homologous end joining and homologous recombination.[26,27] This is interesting given that **RAC1** is not a cross-linking agent. Next, expression of HSP90B1, HSP90 and HSP90 alpha 2 increased upon treatment by 2.1-fold (p<0.007), 1.9-fold (p<0.002) and 1.9-fold (p<0.002) respectively. A recent SILAC experiment revealed their essential role in DNA damage response.[28] Laminin-binding proteins appear to act as adaptors for the chromatin organization, gene expression, epigenetic regulation and modulation of signaling pathways therefore it is not surprising that LGALS3 expression increased threefold due to the large amount of stress cells undergo upon treatment with **RAC1**.[29] Additionally, VIM increased by 2.2 (p<0.02) fold. This protein functions to fortify nuclei structure to maintain survival. Within this set of proteins we noted the key connection between double strand break repair, especially, BRCA1-mediated repair that we will further evaluate directly since many DNA repair proteins are modulated by post-transcriptional modification.

The next two proteins described are involved in stress response and potentially ROS reduction as a means for survival. IRF8 is a key tumor suppressor protein and regulates the expression of BAX and FAS.[30] An increase of 1.7-fold (p>0.009) in TALDO1 (Transaldolase) expression could be beneficial for the cells in two ways. Transaldolase has a well-known role in the pentose phosphate pathway.[31] Up-regulation of this pathway seems to be a critical response since the pentose phosphate pathway synthesizes ribose precursors for DNA synthesis, which would be of obvious benefit to combating the DNA damage function of **RAC1**. The pentose phosphate pathway is known to be activated upstream by ATM phosphorylation, a critical DNA repair protein. Provocatively TALDO1 could also lead to increased glycolysis and NADPH production instead of ROS-generating oxidative phosphorylation.[32] NADPH is a coenzyme for glutathione reductase needed to convert oxidized glutathione (GSSG) to its reduced form (GSH). We have potentially identified an important cellular adaption mechanism that can act as a survival response for AML cancer cells by lowering the activation of **RAC1** and synthesizing more precursors for DNA repair/synthesis.[31] From the proteomics data we obtained two critical responses: increased double strand break repair and movement towards pentose phosphate metabolism to make ribose.

Table 1 *Nuclear Proteins with Altered Expression.*

Protein	*Accession no*	*Fold change*	*ANOVA P*	*Role*
VCP/p97	*gi l 6005942*	*3.4*	*0.002*	*Essential DSBR factor*
LGALS3	*gi l 34234*	*3*	*0.007*	*Adhesion and growth*
CPSF2	*gi l 34101288*	*2.8*	*0.003*	*Pre m-RNA processing*
RPLP0	*gi l 4506667*	*2.4*	*0.001*	*Structural constituent of ribosome*
VIM	*gi l 62414289*	*2.2*	*0.013*	*Nucleus stability*
HSP90B1	*gi l 15010550*	*2.1*	*0.006*	*Chaperone/protein folding*
HSP90	*gi l 306891*	*1.9*	*0.001*	*Chaperone/stabilizes PolB*
HSP90 alpha2	*gi l 61656603*	*1.9*	*0.001*	*Same as above*
TALDO1	*gi l 5803187*	*1.7*	*0.009*	*PPP Metabolism: ribose-phosphate*
HMG-1	*gi | 478813*	*-7.4*	*0.002*	*unknown*
IRF8	*gi | 4504567*	*-1.7*	*0.0001*	*Apoptosis through Bax/Fas*

Transcriptomics of differentially expressed mRNAs upon treatment

RNA-Seq was carried out to characterize the expression of mRNAs upon treatment of **RAC1**. Three treated and three control sample mRNAs were validated for integrity by an Agilent Bioanalyzer 2100. Sequencing results showed over 1000 genes were differentially expressed with p-values less than 0.01 (Figure S3). These genes were analyzed using the ToppGene Suite[33] in order to identify the pathways implicated by the differentially expressed genes. The biological pathways associated with treatment-induced mRNA production changes are summarized in Table 2.

The pathways involved in upregulated mRNAs are described. Out of 1300 genes, 133 (p≤10-29) were involved in the defense response pathway. Also, there were significantly increased transcript levels for genes participating in immune response (126/1416, p≤10-28), response to wounding (101/1255, p≤10-18), regulation of immune system process (96/1212, p≤10-17) and innate immune response (79/883, p≤10-17). For example CREB3L3, CYGB and AQP1 were only expressed upon treatment. These genes are part of stress responses and CYGB is well-known to protect cells exposed to oxidative damage.[34] This implies the involvement of classic ROS/cell damage stress responses upon treatment as immune responses and wound healing involve ROS and cell growth respectively. Interestingly, pathways involving nucleosome assembly (16/143, p≤10-13), chromatin assembly or disassembly (16/182, p≤10-12), nucleosome organization (16/166, p≤10-12) and protein-DNA complex assembly (16/180, p≤10-12) were enriched among downregulated genes, implicating cell cycle arrest as a result of agent treatment as well as the activation of cellular apoptosis as a result of failure of damage repair. Further investigation of expression changes of individual genes involved in DNA damage repair pathway was carried out. Interestingly several poly(ADP-ribose) polymerase (PARP) genes were upregulated. These enzymes are responsible for poly(ADP-ribose) ribose polymerization at DNA damage sites. The identified genes are PARP3, PARP9, PARP10, PARP12, PARP14 and are upregulated by **RAC1** treatment by 2.1, 2.4, 2.0, 3.7 and 1.6 respectively. Though the biological functions of most PARP enzymes are still unknown, a recent study showed that PARP3 has a functional role in DNA repair.[35] It is also reported that PARP12 has a functional role in stress response.[36] Additionally DDB2, (damage specific DNA binding protein 2) expression was upregulated by 2-fold. A major NHEJ pathway protein, XRCC4, mRNA levels were downregulated by 0.5-fold, which is in line with our proteomics that showed BRCA1 mediated responses which are part of a homologous recombination pathway. CDKN1A (p21) expression was up regulated by 7-fold again implicating cell cycle arrest in response to **RAC1**. Further our transcriptomics data showed the upregulation of LGALS3 and VIM and the downregulation of IFR-8 supporting our proteomics data and showing a robust connection between the two techniques. Transcriptomics also showed an increased expression of pentose phosphate pathway enzyme ATP:D-ribose 5-phosphotransferase. Taken together this data correlates with the proteomics data and supports further investigation into the DNA damage response.

Table 2 Biological pathways (fold change>2; p<0.01) from ToppGene analysis.

ID	Name	pValue	Genes from input/genes from Annotation
Up-regulated			
GO:0006952	Defense response	6.517E-30	133/1515
GO:0006955	Immune response	8.569E-29	126/1416
GO:0009611	Response to wounding	1.142E-19	101/1255
GO:0002682	Regulation of immune system process	3.197E-18	96/1212
GO:0045087	Innate immune response	4.817E-18	79/883
Down-regulated			
GO:0006334	Nucleosome assembly	2.078E-14	16/143
GO:0031497	Chromatin assembly	9.157E-14	16/157
GO:0034728	Nucleosome organization	2.201E-13	16/166
GO:0065004	Protein-DNA complex assembly	7.786E-13	16/180

Western blotting to identify double strand break repair mechanism through visualization of post-translational modification signals

Proteomic analysis revealed VCP to increase upon treatment. However, this ATPase has many roles and can eject any polyubiquitinated protein substrate. Thus we wanted to ensure its increase could potentially be involved in DNA repair and chromatin remodeling functions. Western blotting after treatment of AML cells showed an elevation of VCP concentration of 1.37±0.03 fold (p<0.002) within the nucleus but increased expression was not observed in the cytoplasm (p<0.07) (Figure 4A). Thus increased VCP activity may be localized to the nucleus in response to DNA damage necessitating DNA repair and chromatin remodeling.

Double strand break repair is a complex pathway involving mainly homologous recombination (HR) and non-homologous end joining (NHEJ).[37] Following the detection of a double strand break, histone protein H2AX is phosphorylated to form γ-H2AX. This phosphorylation is one of the most common signals for double strand break repair and signals to initiate the repair of double strand breaks. The fate of the double strand break repair pathway will be decided by the enrichment of key proteins, ku70/ku80 and phospho-BRCA1 at the damage sites. Ku80 repair is characteristic of non-homologous end joining, whereas BRCA1 is characteristic of homologous recombination.[38]

In this study, western blot analysis was carried out to quantify the key proteins in the double strand break repair pathway in response to treatment with **RAC1**. The nuclear proteins were extracted after 24 hours of treatment with **RAC1** in AML cells and from mock-treated cells. Figure 4B shows the phosphorylated H2AX variant, γ-H2AX increased 1.9±0.2 fold ($p<0.02$) upon **RAC1** treatment compared to vehicle treatment (Figure 4B). We have also found that treatment of untransformed cells did not show a significant increase (Figure S4). Next we evaluated the phosphorylation status of ATM. This protein not only regulates DNA repair via phosphorylation but also is an obvious link between stress and shunting glycolysis to produce ribose precursors. Western blotting showed an increase of 1.3±0.1 fold ($p<0.04$) in phosphorylation of ATM compared to mock-treated cells (Figure 4C). Upon treatment phosphorylation of ATR significantly increased by 3.1±1.1 fold ($p<0.03$) (Figure 4D) Thus it is clear that DNA double strand break repair is initiated.

To differentiate homologous recombination from non-homologous end joining we chose to investigate the key proteins BRCA1 and ku80. A clear differentiation can be observed by investigating phosphorylation of BRCA1 and the concentration of Ku80 for homologous recombination and not non-homologous end joining respectively. BRCA1 is a promiscuous protein with well-known interactions with RAD51 and other proteins within homologous recombination. Furthermore the activation/phosphorylation of BRCA1 occurs through the auto-phosphorylated ATM after sensing the damaged DNA.[39] The role of Ku80 in the non-homologous end joining is well characterized.[40] Ku complex can bind to the broken end of DNA with high affinity in a sequence independent manner and at the break site it can interact with several factors and enzymes to allow end joining.[41] BRCA1 phosphorylation was enhanced 1.9±0.2 fold ($p<0.05$) upon treatment with **RAC1** (Figure 4E). In contrast, treatment with **RAC1** did not change Ku80 levels within the nucleus as we observed a concentration change of 0.93±0.08 and a p-value of 0.53 (Figure 4F). We conclude that homologous recombination and not non-homologous end joining is the preferred DNA double strand repair mechanism upon treatment with **RAC1**.

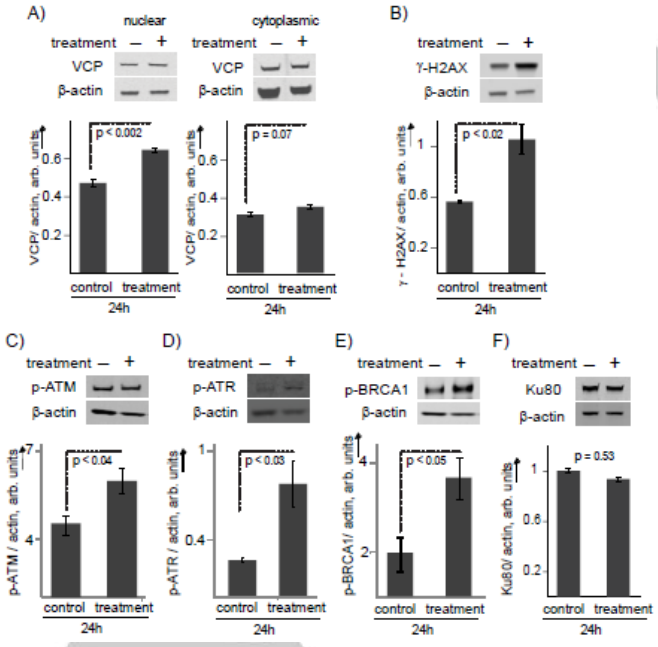

Figure 4. RAC1 induces activation of DNA double strand repair likely through homologous recombination. A) (Left) Western blot of VCP in the nucleus and (Right) in the cytoplasm of AML cells treated with **RAC1** (2 μM) for 24hrs. B) Western blot analysis for γ-H2AX in AML cells C) phosphorylated ATM D) phosphorylated ATR E) phosphorylated BRCA1 and (F) Ku80 in AML cells treated with **RAC1** for 24hrs. Results are presented as means±SEM from biological triplicates.

Synergy with on-pathway compounds

Proteomics, transcriptomics and western blotting indicated a phospho-ATM dependent homologous recombination DNA repair as a key response/survival mechanism of AML cells upon treatment with **RAC1**. Importantly phospho-ATM regulates the identified pentose phosphate pathway and DNA double strand break repair.[42] The standard of care agents also target the DNA repair pathway as daunorubicin will cause DNA double strand breaks and should require phospho-ATM, while cytarabine (AraC) is a multi-modal agent but is thought to principally act by limiting the synthesis of nucleotides needed for DNA synthesis. We therefore expect to see synergy with **RAC1** in combination with specific inhibitors affecting these pathways in AML cells.

Several inhibitors were examined for synergy. KU-55933 was selected since it is a known inhibitor for ATM that limits phosphorylation.[43] VE-821, a potent selective ATP-competitive inhibitor of ATR also examined.[44] In addition we analyzed the DNA damaging agents doxorubicin and cytarabine. The first step in synergy measurements is to elucidate the IC50 values so that dose-effects can be quantified. As such the IC50 values for KU-55933, VE-821, doxorubicin, and cytarabine were 40 μM, 10 μM, 500±5 nM and 1.4±0.2 μM respectively in AML cells. Cells were then treated at doses to elicit ~50% viability with each of these agents, including **RAC1** (Figure 5A). The combinational indexes were calculated using CompuSyn software.[45] As shown in Figure 5A, the combination of **RAC1** and KU-55933 resulted in significant growth inhibition and showed a synergistic effect (CI<1) with a CI value of 0.67. Doxorubicin and cytarabine showed dramatic synergy with the CI values 0.18 and 0.01 respectively. VE-821 showed a strong synergistic effect with a CI value of 0.3. Synergistic effect also investigated in normal CD34+ cells with same inhibitors. In normal cells Ku-55933 and Doxorubicin showed synergy with a CI value of 0.7 and 0.8 respectively. Cytarabine showed a strong synergy with a CI value of 0.18 and VE-821 showed synergy with a CI value of 0.4. Please note that viability in the combination is almost completely lost indicating very apparent synergy. These data strongly show that the synergistic effect of KU-55933, VE-821 and the standard of care compounds doxorubicin and cytarabine, with **RAC1** are specific to transformed AML cells and not CD34+ counter parts. Thus these experiments open the possibility of combinatorial therapy wit **RAC1**.

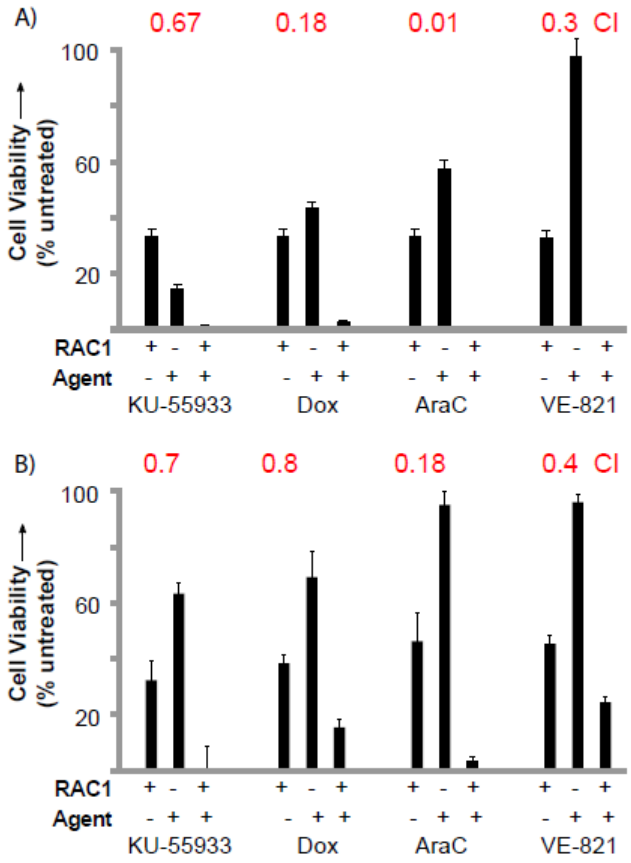

Figure 5. Synergy studies of on pathway inhibitors with **RAC1**. A) AML cells B) Normal CD34+ cells. Cell viability was measured by MTT assay after 48 hours of treatment and compared to IC50 values of single agent treatment for quantification. CI values (red, above) were calculated using CompuSyn software. Results are presented as means±SEM from biological triplicates.

Conclusions

Targeting increased ROS in cancer using ROS-activated agents is a promising new approach that is gaining attraction.[46,47] In this study we report induction of homologous recombination as a predominate mechanism of DNA repair upon treatment with **RAC1**. Proteomics and transcriptomics were used to generate leads regarding the mechanism of action. Interestingly, proteomics of the nuclear fraction led to direct evidence not only of homologous recombination but also activation of the pentose phosphate pathway, which synthesizes ribose for DNA synthesis after repair, consistent with the proposed mechanism. These pathways were further validated by synergy studies. When inhibitors were added at doses that individually had suboptimal effects alone, cells were almost completely eliminated when agents were combined with **RAC1** (compare the bars in Figure 5). Importantly, these effects were specific to cells transformed with MLL-AF9 and FLT3-ITD as untransformed counter parts showed reduced synergy in all cases.

In this manuscript, several important liabilities for poor prognosis AML were observed that we will highlight. Importantly, expression of the oncogenes MLL-AF9 and FLT3-ITD in these cells resulted in enhanced DNA oxidation and reduced anti-oxidant enzymes, which likely leads to a higher mutation rate and potentially more ROS-signalling. We show that RACs exploit this key liability for selective anti-AML activity. Collectively, these data highlight that **RAC1** is able to reach the nucleus, activate via ROS, and cause lethal DNA double strand breaks. These cells entered arrest in the S phase of the replication cycle indicating DNA synthesis is attempted but can not be completed faithfully. Comparing this interesting feature of **RAC1** to literature examples shows this type of genotoxic arrest does occur in some cases with ATR, ATM, and BRCA1 being implicated in the biological mechanism.[48] This is interesting since most of a cell's ROS will be in the mitochondria, endoplasmic reticulum, and cytosol. Despite this modification of DNA is occuring as shown through induction of strand breaks and double strand repair activation. Taken together with our last publication[7] we infer that the formation of adducts at dG, dC, and dA along with a bulky hydroxy-benzethenoguanine adduct (Figure 1) is enough of a challenge to these cells that the lesion is difficult to repair and requires double strand break repair during synthesis. This was validated by quantitative proteomics which gave a strong indication of the mechanism along with RNA-seq results. In addition the proteomics data showed that TALDO1 was increased in response to **RAC1**. This change shows how quickly these AML cells can shift metabolism to generate the ribose-phosphate precursors needed for DNA synthesis after repair (within 24 hrs). The synergy studies, predicated on the findings from our proteomic and transcriptomic analyses, demonstrated strong cooperativity of **RAC1** with standard of care compounds for AML. This study paves the way for in vivo efficacy experiments while at the same time showing that the design of other ROS-activated agents to limit metabolic shifts in cancer cell metabolism may be a promising approach.

Experimental Section

Cell Culture and Cytotoxicity: Human umbilical cord blood (UCB) and transformed AML cells were cultured in IMDM supplemented with 20% FBS.[49] UCB required SCF, IL-3, IL-6, Flt-3L and TPO growth factors at 10 ng/ml. Cytotoxicity analysis as previously described.[6] All R values were greater than 0.98 and standard errors of the three biological replicates were less than 20%. Unless otherwise stated all **RAC1** incubations occurred at 2 μM and for 24 hrs.

Western Blot Analysis: AML cells were grown to a density of $1X10^6$ cells/ml. Samples were treated with **RAC1** for 24 hours. Nuclear protein was extracted using NE-PER (Thermo Scientific) according to the manufacturer's protocol. 10 μg of protein per well was separated by denaturing PAGE gel electrophoresis and transferred onto nitrocellulose membrane using Invitrogen iBlot instrument according to manufacturer's instructions. All western data is expressed as relative to actin. Image analysis was accomplished using a LI-COR imager using standard methods. All fluorescently labeled antibodies were from LI-COR. Assays for catalase was with whole cell lysates.

DCF diacetate fluorescence assay: Cells in active growth phase were pelleted and dissolved in 1X HBSS to a final concentration of $5X10^5$ cells/ml. 100 μl of cells were added to each well in a 96 well plate and incubated in 37˚C, 5% CO_2 for 30 minutes. 100 μl of 1X HBSS was used as blank. Then 100 μl of 20 μM DCF-DA (2',7'-dichlorofluorescein diacetate, DCFH-DA) in 1X HBSS was added to each well. The fluorescence increase was measured (λexc = 485 nm; λem = 535 nm) with a microplate reader after 30 min incubation in 37˚C and 5% CO_2. Care has been taken to control extended light exposure since DCF can undergo light induced oxidation. Data are reported as the mean ± standard deviation of eight replicates. Unpaired t-test was performed to determine the significance.

8-Oxo-7,8-dihydro-2'-deoxyguanosine ELISA assay: Genomic DNA from the UCB and AML cells was isolated using a genomic DNA purification kit (Promega) according to the manufacturer's instructions. Concentration of DNA in each DNA extract was quantified using agarose gel electrophoresis. DNA was digested as described previously.[50] After digestion enzymes were removed by centrifugation and supernatant was used for 8-Oxo-7,8-dihydro-2'-deoxyguanosine quantification using an Oxiselect oxidative DNA damage ELISA kit (Cell Biolabs) according to the manufacturer's instructions.

Apoptosis Assay: Cells were plated and treated with 2 μM **RAC1** or irradiated with 200 mJ/cm^2 UVB. After the desired post-treatment time cells were harvested and stained with APC-Annexin (BD Pharmingen) and propidium iodide (Sigma Chemical). Samples were analyzed by flow cytometry immediately after staining on BD LSR, and the data were analyzed by CELLQuest software.

Single Cell Electrophoresis Assay (Comet Assay): Single-cell electrophoresis was as previously described by Song and colleagues.[51] Briefly, cells were grown to obtain a density of 1X10^6 cells/ml, and treated with 2 μM **RAC1** for 4 hours. As a positive control cells were treated with 105 mJ/cm^2 UVB and incubated for 4 hours. Cells were embedded in 1% low–melting point agarose gel and electrophoresed. The extension of each tail moment, defined as the product of DNA in the tail and the mean distance of its migration, was analyzed using a computerized image analysis system (TriTek CometScore Freeware). The tail moment values obtained from a minimum of 50 randomly selected cells from each slide were expressed as the mean value ± SEM, and data were analyzed by ANOVA ($P \leq 0.05$).

Cell cycle Assay: Cells were plated and treated with 2 μM **RAC1**. After the desired post-treatment time cells were harvested and fixed according to the manufacturer's protocol. BrdU uptake was measured by FACS (FITC BrdU Flow kit, BD Biosciences).

Proteomics: One hundred fifty micrograms of nuclear extracts from three control samples (control) and three experimental samples (treatment) in NE-PER buffer were probe sonicated to shear any residual DNA. Buffer exchange was then performed on the samples with 4 cycles of 100 μL with GE destreak rehydration buffer (GE Healthcare Life Sciences) followed by centrifugation using an Amicon ultra 3kDa centrifugal filter (EMD Millipore). The samples were then loaded in the first dimension on GE 18 cm 3-10NL IPG strips (GE Healthcare Life Sciences) for a total of 57.5 kVhrs. Reduction and alkylation was performed using DTT and iodoacetamide as previously described.[52] The strips were run in the second dimension (12.5% SDS PAGE) at 5 W/gel for 30 min then 17 W/gel until the dye front reached the end of the gel. After fixing and silver staining 16-bit tiff images were obtained. The images were analyzed by Nonlinear Dynamics Progenesis Same Spots software (Durham, NC). The gels were grouped into control vs treatment and automatic spot outlines were manually edited. The software calculates fold change, ANOVA p-value, q value and power for each spot based on all the gels in the experiment. Spots were picked based on having a fold change greater than 1.3, an ANOVA p value < 0.05 and consistency within a group (Power >0.8).

The spots determined to be significantly different between groups were excised from the gel, digested with trypsin (Promega), followed by extraction and desalting, and identification by MALDI TOF-TOF on an ABSCIEX 4800 operated in reflector positive mode all as previously described.22 Proteins were identified by searching the resultant peptide MS/MS sequencing data of the top 20 peptides against the NCBInr homo sapiens database using Mascot software (Matrix Science). Variable modifications of carbamidomethyl cysteine, deamidated asparagine or glutamine, and oxidation of methionine with a maximum of 2 missed cleavages were used. The peptide mass tolerance was set to 125ppm and the fragment mass tolerance to 0.8 Da. A minimum of 2 confident peptides was required for each protein identification reported.

RNA-Seq analysis: After 24 hours of treatment RNA was collected using a total RNA isolation kit (Qiagen). After normalization to 50 ng/μL samples were submitted to the UC Transcriptomics core. At the core facility samples were analyzed for degradation using a bioanalyzer 1200. After validating the integrity, samples were converted to cDNA by using PrepX mRNA Library kit (WaferGen) and Apollo 324 NGS automatic library prep system, and Superscript III reverse transcriptase (Lifetech, Grand Island, NY). Amplified cDNA was quantified using Kapa Library Quantification kit (Kapabiosystem, Woburn, MA) using standard methods and sequence reads were aligned to the genome by using standard Illumina sequence analysis pipeline, which was analyzed by the Statistical Genomics and Systems Biology core in the University of Cincinnati to yield fold-change and anova score. Next, mRNAs with. significant changes (greater than 2-fold and p<0.01) were clustered into pathways using ToppGene [33]

Combination Studies: Response curves, combinational indices, and dose-reduction indices were generated for all treatments and time points with Compusyn® software (Paramus, NJ) according to the manufacturer's instructions and s: Dose dosed as listed. Conditions were the same as cytotoxicity assays.

Acknowledgements

This work is supported by an NIH NCI award (R21CA185370) to E.J.M. The Genomics, Epigenomics and Sequencing Core is supported in part by Center for Environmental Genetics grant (NIEHS P30-ES006096). We would also like to thank an Institutional Clinical and Translational Science Award, NIH/NCR R Grant Number 1UL1RR026314-01. This work was supported by a Translational Trials Development and Support Laboratory award (USPHS, MO1 RR 08084) and a Center of Excellence in Molecular Hematology P30 award (DK090971) to J.C.M. J.C.M. is a Leukemia and Lymphoma Society Scholar. This work was further supported by through the University of Cincinnati Millennium Scholar Fund and the Cincinnati Children's Research Foundation to K.D.G.

Keywords: ROS, acute myeloid leukemia, homologous recombination, mechanism of action, MLL-AF9

[1] N. Shrivastav, D. Y. Li, J. M. Essigmann, *Carcinogenesis* **2010**, *31*, 59-70
[2] N. P. Shah, C. Tran, F. Y. Lee, P. Chen, D. Norris, C. L. Sawyers, *Science* **2004**, *305*, 399-401.
[3] M. M. Greenberg, *Curr. Opin. Chem. Biol.* **2014**, *21*, 48-55.
[4] P. L. McKibbin, A. M. Fleming, M. A. Towheed, B. Van Houten, C. J. Burrows, S. S. David, *Journal of the American Chemical Society* **2013**, *135*, 13851-13861.
[5] A. M. Wu, P. D. Senter, *Nature Biotechnology* **2005**, *23*, 1137-1146.
[6] T. R. Bell-Horwath, A. K. Vadukoot, F. S. Thowfeik, G. Li, M. Wunderlich, J. C. Mulloy, E. J. Merino, *Bioorganic & Medicinal Chemistry Letters* **2013**, *23*, 2951-2954.
[7] A. R. Jones, T. R. Bell-Horwath, G. Li, S. M. Rollmann, E. J. Merino, *Chemical Research in Toxicology* **2012**, *25*, 2542-2552.
[8] Y. H. Siddique, G. Ara, T. Beg, J. Gupta, M. Afzal, *Experimental and Toxicologic Pathology* **2010**, *62*, 503-508.
[9] L. C. Colis, C. M. Woo, D. C. Hegan, Z. W. Li, P. M. Glazer, S. B. Herzon, *Nature Chemistry* **2014**, *6*, 504-510.
[10] S. S. Pei, M. Minhajuddin, K. P. Callahan, M. Balys, J. M. Ashton, S. J. Neering, E. D. Lagadinou, C. Corbett, H. B. Ye, J. L. Liesveld, K. M. O'Dwyer, Z. Li, L. Shi, P. Greninger, J. Settleman, C. Benes, F. K. Hagen, J. Munger, P. A. Crooks, M. W. Becker, C. T. Jordan, *Journal of Biological Chemistry* **2013**, *288*, 33542-33558.
[11] R. Godfrey, D. Arora, R. Bauer, S. Stopp, J. P. Mueller, T. Heinrich, S.-A. Boehmer, M. Dagnell, U. Schnetzke, S. Scholl, A. Ostman, F.-D. Boehmer, *Blood* **2012**, *119*, 4499-4511.
[12] P. S. Hole, J. Zabkiewicz, C. Munje, Z. Newton, L. Pearn, P. White, N. Marquez, H. R.K., A. K. Burnett, A. Tonks, R. L. Darley, *Blood* **2013**, *Accepted*, 10.1182/blood-2013-1104-491944.
[13] M. E. Irwin, N. Rivera-Del Valle, J. Chandra, *Antioxidants & Redox Signaling* **2013**, *18*, 1349-1383.
[14] Y. Hu, W. Lu, G. Chen, P. Wang, Z. Chen, Y. Zhou, M. Ogasawara, D. Trachootham, L. Feng, H. Pelicano, P. J. Chiao, M. J. Keating, G. Garcia-Manero, P. Huang, *Cell Research* **2012**, *22*, 399-412.
[15] M. M. Reddy, M. S. Fernandes, R. Salgia, R. L. Levine, J. D. Griffin, M. Sattler, *Leukemia* **2011**, *25*, 281-289.
[16] A. Sallmyr, J. Fan, K. Datta, K.-T. Kim, D. Grosu, P. Shapiro, D. Small, F. Rassool, *Blood* **2008**, *111*, 3173-3182.
[17] K. Ke, O. J. Sul, E. K. Choi, A. M. Safdar, E. S. Kim, H. S. Choi, *Am. J. Physiol.-Endocrinol. Metab.* **2014**, *307*, E61-E70.
[18] Q. S. Zhu, L. Xia, G. B. Mills, C. A. Lowell, I. P. Touw, S. J. Corey, *Blood* **2006**, *107*, 1847-1856.
[19] M. Wunderlich, B. Mizukawa, F. S. Chou, C. Sexton, M. Shrestha, Y. Saunthararajah, J. C. Mulloy, *Blood* **2013**, *121*, e90-97.
[20] F. O. Bagger, N. Rapin, K. Theilgaard-Monch, B. Kaczkowski, L. A. Thoren, J. Jendholm, O. Winther, B. T. Porse, *Nucleic Acids Res* **2013**, *41*, D1034-1039.
[21] S. Yamamoto, Y. Tomita, S. Nakamori, Y. Hoshida, H. Nagano, K. Dono, K. Umeshita, M. Sakon, M. Monden, K. Aozasa, *J Clin Oncol* **2003**, *21*, 447-452.

[22] Y. Tsujimoto, Y. Tomita, Y. Hoshida, T. Kono, T. Oka, S. Yamamoto, N. Nonomura, A. Okuyama, K. Aozasa, *Clinical Cancer Research* **2004**, *10*, 3007-3012.

[23] R. M. Dai, E. Chen, D. L. Longo, C. M. Gorbea, C. C. Li, *J Biol Chem* **1998**, *273*, 3562-3573.

[24] T. Asai, Y. Tomita, S.-i. Nakatsuka, Y. Hoshida, A. Myoui, H. Yoshikawa, K. Aozasa, *Cancer Science* **2002**, *93*, 296-304.

[25] P. Magnaghi, R. D'Alessio, B. Valsasina, N. Avanzi, S. Rizzi, D. Asa, F. Gasparri, L. Cozzi, U. Cucchi, C. Orrenius, P. Polucci, D. Ballinari, C. Perrera, A. Leone, G. Cervi, E. Casale, Y. Xiao, C. Wong, D. J. Anderson, A. Galvani, D. Donati, T. O'Brien, P. K. Jackson, A. Isacchi, *Nat Chem Biol* **2013**, *9*, 548-556.

[26] N. P. Dantuma, K. Acs, M. S. Luijsterburg, *Exp Cell Res* **2014**, *329*, 9-17.

[27] M. S. Luijsterburg, H. van Attikum, *Current Opinion in Cell Biology* **2012**, *24*, 439-447.

[28] K. Sharma, R. M. Vabulas, B. Macek, S. Pinkert, J. Cox, M. Mann, F. U. Hartl, *Mol Cell Proteomics* **2012**, *11*, M111.014654.

[29] K. L. Wilson, R. Foisner, *Cold Spring Harb Perspect Biol* **2010**, *2*, a000554.

[30] J. Yang, X. Hu, M. Zimmerman, C. M. Torres, D. Yang, S. B. Smith, K. Liu, *J Immunol* **2011**, *187*, 4426-4430.

[31] A. Perl, R. Hanczko, T. Telarico, Z. Oaks, S. Landas, *Trends Mol Med* **2011**, *17*, 395-403.

[32] V. Sosa, T. Moline, R. Somoza, R. Paciucci, H. Kondoh, L. L. ME, *Ageing Res Rev* **2013**, *12*, 376-390.

[33] J. Chen, E. E. Bardes, B. J. Aronow, A. G. Jegga, *Nucleic Acids Research* **2009**, *37*, W305-W311.

[34] L. T. T. Thuy, Y. Matsumoto, T. T. V. Thuy, H. Hai, M. Suoh, Y. Urahara, H. Motoyama, H. Fujii, A. Tamori, S. Kubo, S. Takemura, T. Morita, K. Yoshizato, N. Kawada, *The American Journal of Pathology*, *185*, 1045-1060.

[35] C. Boehler, L. R. Gauthier, O. Mortusewicz, D. S. Biard, J.-M. Saliou, A. Bresson, S. Sanglier-Cianferani, S. Smith, V. Schreiber, F. Boussin, F. Dantzer, *Proceedings of the National Academy of Sciences* **2011**, *108*, 2783-2788;

[36] I. Welsby, D. Hutin, C. Gueydan, V. Kruys, A. Rongvaux, O. Leo, *Journal of Biological Chemistry* **2014**, *289*, 26642-26657.

[37] J. R. Chapman, M. R. Taylor, S. J. Boulton, *Mol Cell* **2012**, *47*, 497-510.

[38] M. Srivastava, S. C. Raghavan, *Chem Biol* **2015**, *22*, 17-29.

[39] F. Gullotta, E. De Marinis, P. Ascenzi, A. di Masi, *Curr Med Chem* **2010**, *17*, 2017-2048.

[40] V. L. Fell, C. Schild-Poulter, *Mutation Research/Reviews in Mutation Research* **2015**, *763*, 15-29.

[41] C. Moon, H. Y. Moon, C. S. Kim, *Korean J Urol* **2007**, *48*, 976-983.

[42] E. Tsouko, A. S. Khan, M. A. White, J. J. Han, Y. Shi, F. A. Merchant, M. A. Sharpe, L. Xin, D. E. Frigo, *Oncogenesis* **2014**, *3*, e103.

[43] I. Hickson, Y. Zhao, C. J. Richardson, S. J. Green, N. M. Martin, A. I. Orr, P. M. Reaper, S. P. Jackson, N. J. Curtin, G. C. Smith, *Cancer Res* **2004**, *64*, 9152-9159.

[44] P. M. Reaper, M. R. Griffiths, J. M. Long, J. D. Charrier, S. Maccormick, P. A. Charlton, J. M. Golec, J. R. Pollard, *Nat Chem Biol* **2011**, *7*, 428-430.

[45] T.-C. Chou, *Cancer Research* **2010**, *70*, 440-446.

[46] X. Peng, V. Gandhi, *Therapeutic Delivery* **2012**, *3*, 823-833.

[47] W. Chen, K. Balakrishnan, Y. Kuang, Y. Han, M. Fu, V. Gandhi, X. Peng, *J Med Chem* **2014**, *57*, 4498-4510.

[48] J. Bartek, C. Lukas, J. Lukas, *Nat Rev Mol Cell Biol.* **2004**, 5, 792-804.

[49] J. C. Mulloy, J. Cammenga, K. L. MacKenzie, F. J. Berguido, M. A. Moore, S. D. Nimer, *Blood* **2002**, *99*, 15-23.

[50] G. Boysen, L. B. Collins, S. Liao, A. M. Luke, B. F. Pachkowski, J. L. Watters, J. A. Swenberg, *J Chromatogr B Analyt Technol Biomed Life Sci* **2010**, *878*, 375-380.

[51] X. Song, N. Mosby, J. Yang, A. Xu, Z. Abdel-Malek, A. L. Kadekaro, *Pigment Cell & Melanoma Research* **2009**, *22*, 809-818.

[52] T. Eismann, N. Huber, T. Shin, S. Kuboki, E. Galloway, M. Wyder, M. J. Edwards, K. D. Greis, H. G. Shertzer, A. B. Fisher, A. B. Lentsch, *Am J Physiol Gastrointest Liver Physiol* **2009**, *296*, G266-274.

Text for Table of Contents

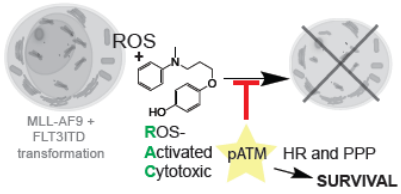

Fathima Shazna Thowfeik[a], Safnas F. AbdulSalam[a], Mark Wunderlich[b], Michael Wyder[d], Kenneth D. Greis[d], Ana L. Kadekaro[c], James C. Mulloy[b], Edward J. Merino[a]

Page No. – Page No.

A ROS-activatable agent elicits homologous recombination DNA repair and synergizes with pathway compounds.

Supporting Information

Table of Contents

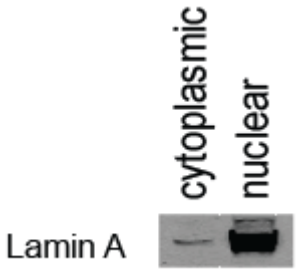

Figure S1. Example of nuclear protein extraction. Nuclear isolation enriches the nuclear marker, lamin A, by 9-fold.

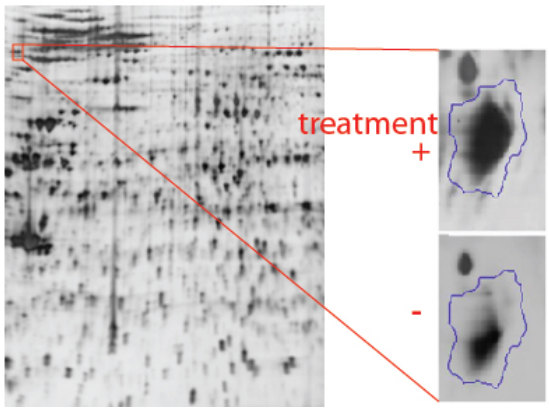

Figure S2. Example 2D gel of isolated nuclei. Nuclei from AML cell lines were isolated after treatment or control. An example a treatment gel is shown. Normalized protein was separated by 2D gel electrophoresis and quantified. The box region is enlarged and shown in both a treated and control sample gel image. Statistically different spots were identified.

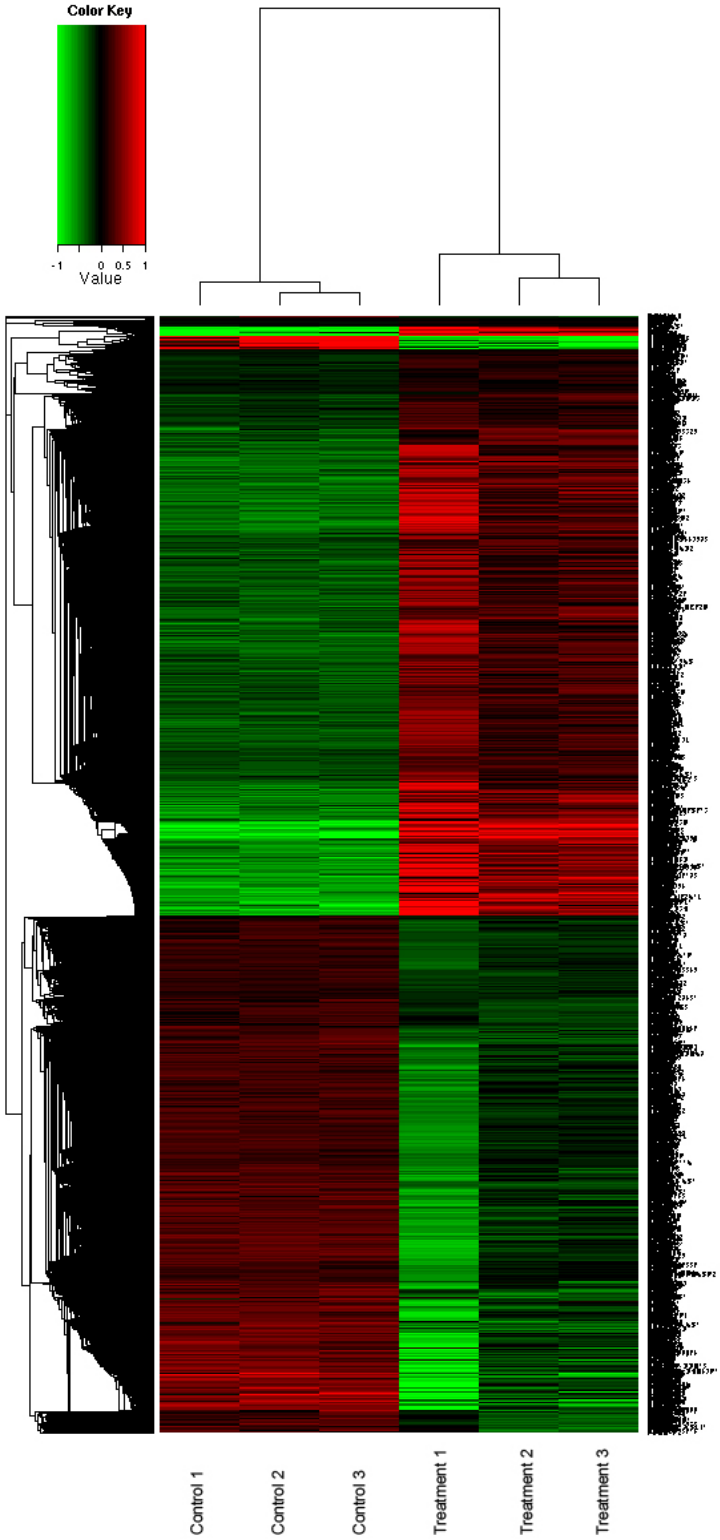

Figure S3. Expression changes upon treatment. RNA-seq heat map.

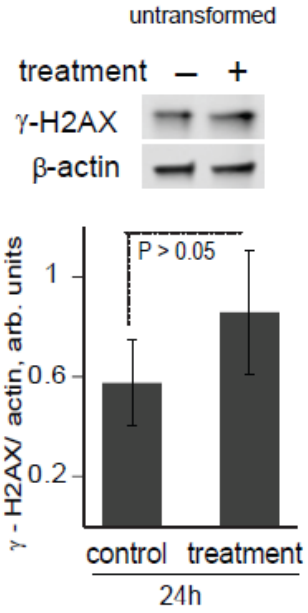

Figure S4. Western blot analysis for γ-H2AX in untransformed cells.

Gene id	Symbol	Name	Base Mean	Base Mean RAC1	Base Mean Control	Fold Change	p-value
151887	CCDC80	coiled-coil domain containing 80	6.533	13.067	A	A	0.000
84699	CREB3L3	cAMP responsive element bindingprotein 3-like 3	6.009	12.018	A	A	0.000
114757	CYGB	cytoglobin	3.917	7.834	A	A	0.001
29094	LGALSL	lectin, galactoside-binding-like	3.838	7.676	A	A	0.002
23604	DAPK2	death-associated protein kinase 2	3.152	6.304	A	A	0.004
358	AQP1	aquaporin 1 (Colton blood group)	2.913	5.827	A	A	0.007
1E+08	GAGE12D	G antigen 12D	4.286	8.572	A	A	0.012
729422	GAGE12C	G antigen 12C	4.286	8.572	A	A	0.012
729431	GAGE12E	G antigen 12E	4.286	8.572	A	A	0.012
7053	TGM3	transglutaminase 3 (E polypeptide, protein-glutamine-gamma-glutamyltransferase)	6.767	13.236	0.298	0.023	0.000
3891	KRT85	keratin 85	6.518	12.738	0.298	0.023	0.002
81029	WNT5B	wingless-type MMTV integration site family, member 5B	6.005	11.695	0.315	0.027	0.000
4855	NOTCH4	notch 4	4.761	9.224	0.298	0.032	0.001
2066	ERBB4	v-erb-a erythroblastic leukemia viral oncogene homolog 4 (avian)	4.287	8.258	0.315	0.038	0.004
9853	RUSC2	RUN and SH3 domain containing 2	8.285	15.955	0.614	0.038	0.000
3001	GZMA	granzyme A (granzyme 1, cytotoxic T-lymphocyte-associated serine esterase 3)	5.054	9.731	0.378	0.039	0.001
6678	SPARC	secreted protein, acidic, cysteine-rich (osteonectin)	16.929	32.568	1.290	0.040	0.000
923	CD6	CD6 molecule	10.567	20.221	0.912	0.045	0.000
1769	DNAH8	dynein, axonemal, heavy chain 8	6.832	13.067	0.597	0.046	0.000
3250	HPR	haptoglobin-related protein	36.804	70.364	3.245	0.046	0.000
7498	XDH	xanthine dehydrogenase	7.482	14.288	0.676	0.047	0.000
3887	KRT81	keratin 81	39.979	76.133	3.825	0.050	0.000
4318	MMP9	matrix metallopeptidase 9 (gelatinase B, 92kDa gelatinase, 92kDa type IV collagenase)	76.585	144.888	8.282	0.057	0.000
6402	SELL	selectin L	8.183	15.471	0.895	0.058	0.000

1E+08	NA	NA	11.605	21.903	1.307	0.060	0.000
120892	LRRK2	leucine-rich repeat kinase 2	260.982	491.915	30.049	0.061	0.000
80183	KIAA0226L	KIAA0226-like	38.756	73.028	4.484	0.061	0.000
3240	HP	haptoglobin	220.690	412.863	28.518	0.069	0.000
3892	KRT86	keratin 86	118.574	221.725	15.424	0.070	0.000
9381	OTOF	otoferlin	5.094	9.512	0.676	0.071	0.003
4151	MB	myoglobin	4.596	8.579	0.614	0.072	0.007
1E+08	NA	NA	4.459	8.322	0.597	0.072	0.007
8557	TCAP	titin-cap	7.060	13.146	0.975	0.074	0.000
115350	FCRL1	Fc receptor-like 1	58.052	108.061	8.044	0.074	0.000
27299	ADAMDEC1	ADAM-like, decysin 1	19.910	36.877	2.943	0.080	0.000
23569	PADI4	peptidyl arginine deiminase, type IV	411.646	761.718	61.575	0.081	0.000
2191	FAP	fibroblast activation protein, alpha	12.050	22.276	1.825	0.082	0.000
5551	PRF1	perforin 1 (pore forming protein)	6.751	12.448	1.054	0.085	0.001
9935	MAFB	v-maf musculoaponeurotic fibrosarcoma oncogene homolog B (avian)	85.072	156.330	13.815	0.088	0.000
7057	THBS1	thrombospondin 1	130.334	238.475	22.193	0.093	0.000
6474	SHOX2	short stature homeobox 2	9.686	17.722	1.651	0.093	0.000
4192	MDK	midkine (neurite growth-promoting factor 2)	7.073	12.918	1.228	0.095	0.002
10842	PPP1R17	protein phosphatase 1, regulatory subunit 17	16.156	29.478	2.835	0.096	0.000
9447	AIM2	absent in melanoma 2	23.097	42.121	4.073	0.097	0.000
162461	TMEM92	transmembrane protein 92	11.615	21.167	2.063	0.097	0.000
671	BPI	bactericidal/permeability-increasing protein	22.010	40.054	3.966	0.099	0.000
56243	KIAA1217	KIAA1217	23.990	43.630	4.350	0.100	0.000
4648	MYO7B	myosin VIIB	33.631	61.096	6.165	0.101	0.000
3889	KRT83	keratin 83	13.584	24.650	2.518	0.102	0.001
347	APOD	apolipoprotein D	17.379	31.518	3.239	0.103	0.000
2312	FLG	filaggrin	35.639	64.534	6.744	0.105	0.000
343521	TCTEX1D4	Tctex1 domain containing 4	7.048	12.743	1.352	0.106	0.003
719	C3AR1	complement component 3a receptor 1	97.582	176.403	18.761	0.106	0.000
7123	CLEC3B	C-type lectin domain family 3, member B	7.872	14.218	1.526	0.107	0.006
4808	NHLH2	nescient helix loop helix 2	9.550	17.197	1.904	0.111	0.008

148113	CILP2	cartilage intermediate layer protein 2	15.657	28.183	3.132	0.111	0.000
8876	VNN1	vanin 1	208.489	375.154	41.824	0.111	0.000
2357	FPR1	formyl peptide receptor 1	56.474	101.521	11.427	0.113	0.000
6274	S100A3	S100 calcium binding protein A3	13.850	24.884	2.816	0.113	0.000
79782	LRRC31	leucine rich repeat containing 31	14.902	26.687	3.117	0.117	0.000
3680	ITGA9	integrin, alpha 9	5.829	10.414	1.245	0.120	0.008
199713	NLRP7	NLR family, pyrin domain containing 7	23.819	42.398	5.240	0.124	0.000
4051	CYP4F3	cytochrome P450, family 4, subfamily F, polypeptide 3	15.117	26.898	3.336	0.124	0.000
1E+08	NA	NA	8.395	14.901	1.889	0.127	0.001
10804	GJB6	gap junction protein, beta 6, 30kDa	8.936	15.843	2.029	0.128	0.001
57664	PLEKHA4	pleckstrin homology domain containing, family A (phosphoinositide binding specific) member 4	7.416	13.102	1.730	0.132	0.002
164668	APOBEC3H	apolipoprotein B mRNA editing enzyme, catalytic polypeptide-like 3H	64.094	113.221	14.967	0.132	0.000
91523	PCED1B	PC-esterase domain containing 1B	18.118	32.005	4.231	0.132	0.000
53829	P2RY13	purinergic receptor P2Y, G-protein coupled, 13	17.173	30.328	4.017	0.132	0.000
4973	OLR1	oxidized low density lipoprotein (lectin-like) receptor 1	14.235	25.118	3.353	0.133	0.001
440073	IQSEC3	IQ motif and Sec7 domain 3	9.237	16.288	2.185	0.134	0.001
366	AQP9	aquaporin 9	13.842	24.364	3.321	0.136	0.001
2857	GPR34	G protein-coupled receptor 34	54.176	95.265	13.086	0.137	0.000
1284	COL4A2	collagen, type IV, alpha 2	11.596	20.375	2.818	0.138	0.002
3101	HK3	hexokinase 3 (white cell)	653.904	1145.22	162.585	0.142	0.000
2219	FCN1	ficolin (collagen/fibrinogen domain containing) 1	90.345	158.200	22.490	0.142	0.000
10461	MERTK	c-mer proto-oncogene tyrosine kinase	15.093	26.395	3.791	0.144	0.000
286749	STON1-GTF2A1L	STON1-GTF2A1L readthrough	109.996	192.111	27.880	0.145	0.000
1E+08	GDNF-AS1	GDNF antisense RNA 1 (head to head)	5.696	9.944	1.449	0.146	0.009

1E+08	NA	NA	9.243	16.108	2.378	0.148	0.001
1026	CDKN1A	cyclin-dependent kinase inhibitor 1A (p21, Cip1)	3456.8	6021.21	892.387	0.148	0.000
3672	ITGA1	integrin, alpha 1	59.059	102.784	15.333	0.149	0.000
941	CD80	CD80 molecule	24.652	42.894	6.410	0.149	0.000
246	ALOX15	arachidonate 15-lipoxygenase	24.554	42.720	6.388	0.150	0.000
1E+08	NA	NA	14.058	24.439	3.678	0.150	0.000
8291	DYSF	dysferlin, limb girdle muscular dystrophy 2B (autosomal recessive)	28.768	49.917	7.619	0.153	0.000
1E+08	LOC100507600	uncharacterized LOC100507600	42.408	73.538	11.278	0.153	0.000
283491	OR7E156P	olfactory receptor, family 7, subfamily E, member 156 pseudogene	5.991	10.377	1.605	0.155	0.011
79778	MICALL2	MICAL-like 2	37.633	65.022	10.243	0.158	0.001
3675	ITGA3	integrin, alpha 3 (antigen CD49C, alpha 3 subunit of VLA-3 receptor)	6.011	10.371	1.651	0.159	0.011
25984	KRT23	keratin 23 (histone deacetylase inducible)	52.003	89.641	14.365	0.160	0.000
5617	PRL	prolactin	93.119	160.477	25.760	0.161	0.000
64411	ARAP3	ArfGAP with RhoGAP domain, ankyrin repeat and PH domain 3	39.266	67.576	10.957	0.162	0.000
1191	CLU	clusterin	45.797	78.750	12.844	0.163	0.000
5332	PLCB4	phospholipase C, beta 4	67.069	115.254	18.884	0.164	0.000
11037	STON1	stonin 1	244.288	418.759	69.817	0.167	0.000
25780	RASGRP3	RAS guanyl releasing protein 3 (calcium and DAG-regulated)	14.111	24.068	4.154	0.173	0.000
338440	ANO9	anoctamin 9	6.618	11.286	1.949	0.173	0.010
1289	COL5A1	collagen, type V, alpha 1	15.719	26.745	4.693	0.175	0.001
1057	CELP	carboxyl ester lipase pseudogene	15.752	26.773	4.732	0.177	0.000
56670	SUCNR1	succinate receptor 1	1120.4	1903.95	336.999	0.177	0.000
115019	SLC26A9	solute carrier family 26, member 9	12.838	21.806	3.870	0.177	0.001
3162	HMOX1	heme oxygenase (decycling) 1	59.046	100.284	17.809	0.178	0.009
6708	SPTA1	spectrin, alpha, erythrocytic 1 (elliptocytosis 2)	7.883	13.370	2.395	0.179	0.006
340206	TREML3P	triggering receptor expressed on myeloid cells-like 3, pseudogene	9.290	15.717	2.864	0.182	0.002

55301	OLAH	oleoyl-ACP hydrolase	341.944	577.458	106.431	0.184	0.000
54209	TREM2	triggering receptor expressed on myeloid cells 2	37.697	63.518	11.875	0.187	0.000
125336	LOXHD1	lipoxygenase homology domains 1	240.025	404.190	75.861	0.188	0.000
909	CD1A	CD1a molecule	14.942	25.149	4.734	0.188	0.000
644100	ARL14EPL	ADP-ribosylation factor-like 14 effector protein-like	10.060	16.927	3.194	0.189	0.003
1E+08	LOC100507195	uncharacterized LOC100507195	15.713	26.433	4.992	0.189	0.000
1E+08	LOC100506115	uncharacterized LOC100506115	16.798	28.245	5.351	0.189	0.000
1893	ECM1	extracellular matrix protein 1	814.349	1368.26	260.430	0.190	0.000
6283	S100A12	S100 calcium binding protein A12	370.554	622.568	118.539	0.190	0.000
55930	MYO5C	myosin VC	42.393	71.199	13.586	0.191	0.000
718	C3	complement component 3	449.622	754.567	144.676	0.192	0.000
969	CD69	CD69 molecule	275.873	462.656	89.090	0.193	0.000
1056	CEL	carboxyl ester lipase (bile salt-stimulated lipase)	37.633	63.093	12.174	0.193	0.000
8807	IL18RAP	interleukin 18 receptor accessory protein	230.434	385.459	75.410	0.196	0.000
6286	S100P	S100 calcium binding protein P	64.748	108.284	21.212	0.196	0.000
4308	TRPM1	transient receptor potential cation channel, subfamily M, member 1	14.588	24.394	4.783	0.196	0.001
3957	LGALS2	lectin, galactoside-binding, soluble, 2	44.655	74.635	14.675	0.197	0.000
6272	SORT1	sortilin 1	239.198	399.009	79.387	0.199	0.000
6285	S100B	S100 calcium binding protein B	102.542	170.824	34.259	0.201	0.000
1674	DES	desmin	52.002	86.290	17.714	0.205	0.000
5806	PTX3	pentraxin 3, long	157.710	261.690	53.730	0.205	0.000
8875	VNN2	vanin 2	32.223	53.445	11.001	0.206	0.000
8991	SELENBP1	selenium binding protein 1	33.093	54.871	11.316	0.206	0.000
1E+08	NA	NA	7.770	12.881	2.659	0.206	0.010
1572	CYP2F1	cytochrome P450, family 2, subfamily F, polypeptide 1	8.498	14.066	2.929	0.208	0.008
768206	PRCD	progressive rod-cone degeneration	9.182	15.198	3.165	0.208	0.006
53826	FXYD6	FXYD domain containing ion transport regulator 6	50.334	83.292	17.375	0.209	0.000
6948	TCN2	transcobalamin II	68.345	112.990	23.701	0.210	0.000

50615	IL21R	interleukin 21 receptor	210.156	347.353	72.959	0.210	0.000
116071	BATF2	basic leucine zipper transcription factor, ATF-like 2	8.231	13.601	2.862	0.210	0.010
8857	FCGBP	Fc fragment of IgG binding protein	104.684	172.956	36.412	0.211	0.000
2358	FPR2	formyl peptide receptor 2	894.511	1475.85	313.170	0.212	0.000
929	CD14	CD14 molecule	447.103	737.194	157.012	0.213	0.000
57576	KIF17	kinesin family member 17	11.906	19.615	4.197	0.214	0.007
55026	TMEM255A	transmembrane protein 255A	34.072	55.990	12.154	0.217	0.000
28514	DLL1	delta-like 1 (Drosophila)	11.523	18.903	4.142	0.219	0.003
64753	CCDC136	coiled-coil domain containing 136	17.848	29.274	6.422	0.219	0.000
23612	PHLDA3	pleckstrin homology-like domain, family A, member 3	82.383	134.877	29.889	0.222	0.000
653361	NCF1	neutrophil cytosolic factor 1	351.364	575.206	127.522	0.222	0.003
2012	EMP1	epithelial membrane protein 1	232.888	381.216	84.560	0.222	0.000
81607	PVRL4	poliovirus receptor-related 4	38.643	63.146	14.139	0.224	0.000
389118	CDHR4	cadherin-related family member 4	13.391	21.826	4.956	0.227	0.002
6947	TCN1	transcobalamin I (vitamin B12 binding protein, R binder family)	149.098	242.972	55.224	0.227	0.000
6640	SNTA1	syntrophin, alpha 1	9.409	15.309	3.509	0.229	0.008
3976	LIF	leukemia inhibitory factor	37.561	61.079	14.043	0.230	0.000
2633	GBP1	guanylate binding protein 1, interferon-inducible	38.300	62.273	14.326	0.230	0.000
355	FAS	Fas (TNF receptor superfamily, member 6)	137.573	223.581	51.565	0.231	0.000
1277	COL1A1	collagen, type I, alpha 1	48.302	78.428	18.175	0.232	0.010
339400	FLG-AS1	FLG antisense RNA 1	11.116	18.030	4.203	0.233	0.005
10863	ADAM28	ADAM metallopeptidase domain 28	37.358	60.583	14.134	0.233	0.000
6368	CCL23	chemokine (C-C motif) ligand 23	54.340	88.041	20.638	0.234	0.000
3983	ABLIM1	actin binding LIM protein 1	22.689	36.752	8.626	0.235	0.000
5003	SLC22A18AS	solute carrier family 22 (organic cation transporter), member 18 antisense	24.738	40.035	9.442	0.236	0.000
128506	OCSTAMP	osteoclast stimulatory transmembrane protein	13.155	21.244	5.066	0.238	0.002
3075	CFH	complement factor H	17.919	28.927	6.911	0.239	0.001

641700	ECSCR	endothelial cell surface expressed chemotaxis and apoptosis regulator	24.095	38.888	9.302	0.239	0.000
79083	MLPH	melanophilin	209.700	338.183	81.218	0.240	0.000
597	BCL2A1	BCL2-related protein A1	135.174	217.965	52.383	0.240	0.000
58476	TP53INP2	tumor protein p53 inducible nuclear protein 2	561.748	905.718	217.778	0.240	0.000
8794	TNFRSF10C	tumor necrosis factor receptor superfamily, member 10c, decoy without an intracellular domain	8.390	13.522	3.258	0.241	0.011
654817	NCF1C	neutrophil cytosolic factor 1C pseudogene	335.753	540.070	131.436	0.243	0.003
1043	CD52	CD52 molecule	297.309	478.043	116.575	0.244	0.008
2208	FCER2	Fc fragment of IgE, low affinity II, receptor for (CD23)	486.593	780.709	192.477	0.247	0.000
388697	HRNR	hornerin	36.852	59.089	14.615	0.247	0.000
115653	KIR3DL3	killer cell immunoglobulin-like receptor, three domains, long cytoplasmic tail, 3	9.391	15.052	3.730	0.248	0.010
8544	PIR	pirin (iron-binding nuclear protein)	34.854	55.844	13.864	0.248	0.000
9881	TRANK1	tetratricopeptide repeat and ankyrin repeat containing 1	318.727	510.418	127.037	0.249	0.000
284417	TMEM150B	transmembrane protein 150B	30.456	48.726	12.186	0.250	0.000
115362	GBP5	guanylate binding protein 5	158.405	253.243	63.568	0.251	0.000
25903	OLFML2B	olfactomedin-like 2B	28.094	44.890	11.299	0.252	0.000
84658	EMR3	egf-like module containing, mucin-like, hormone receptor-like 3	18.436	29.414	7.459	0.254	0.001
79168	LILRA6	leukocyte immunoglobulin-like receptor, subfamily A (with TM domain), member 6	728.551	1162.32	294.781	0.254	0.000
55655	NLRP2	NLR family, pyrin domain containing 2	187.582	299.172	75.991	0.254	0.000
2686	GGT7	gamma-glutamyltransferase 7	13.935	22.210	5.661	0.255	0.003
80737	VWA7	von Willebrand factor A domain containing 7	19.041	30.324	7.757	0.256	0.001
201456	FBXO15	F-box protein 15	34.904	55.586	14.223	0.256	0.000
55561	CDC42BPG	CDC42 binding protein kinase gamma (DMPK-like)	9.240	14.704	3.776	0.257	0.010

79625	NDNF	neuron-derived neurotrophic factor	112.407	178.744	46.070	0.258	0.000
1E+08	ZNF503-AS2	ZNF503 antisense RNA 2	27.420	43.583	11.257	0.258	0.000
4818	NKG7	natural killer cell group 7 sequence	472.068	749.895	194.241	0.259	0.000
8638	OASL	2'-5'-oligoadenylate synthetase-like	48.075	76.367	19.783	0.259	0.000
9289	GPR56	G protein-coupled receptor 56	24.275	38.544	10.007	0.260	0.000
1E+08	PIR-FIGF	PIR-FIGF readthrough	23.818	37.816	9.820	0.260	0.000
339665	SLC35E4	solute carrier family 35, member E4	15.306	24.301	6.311	0.260	0.002
10580	SORBS1	sorbin and SH3 domain containing 1	12.609	20.007	5.211	0.260	0.006
222487	GPR97	G protein-coupled receptor 97	142.700	226.306	59.094	0.261	0.000
5199	CFP	complement factor properdin	275.958	436.384	115.532	0.265	0.000
10170	DHRS9	dehydrogenase/reductase (SDR family) member 9	1249.03	1974.46	523.600	0.265	0.000
3108	HLA-DMA	major histocompatibility complex, class II, DM alpha	56.576	89.356	23.797	0.266	0.000
3127	HLA-DRB5	major histocompatibility complex, class II, DR beta 5	118.443	186.971	49.914	0.267	0.000
116379	IL22RA2	interleukin 22 receptor, alpha 2	52.016	82.108	21.925	0.267	0.000
2051	EPHB6	EPH receptor B6	24.981	39.420	10.542	0.267	0.000
64761	PARP12	poly (ADP-ribose) polymerase family, member 12	117.745	185.706	49.784	0.268	0.000
654816	NCF1B	neutrophil cytosolic factor 1B pseudogene	316.273	498.560	133.986	0.269	0.001
27123	DKK2	dickkopf 2 homolog (Xenopus laevis)	21.857	34.449	9.265	0.269	0.000
79007	DBNDD1	dysbindin (dystrobrevin binding protein 1) domain containing 1	33.809	53.266	14.351	0.269	0.000
10234	LRRC17	leucine rich repeat containing 17	26.513	41.695	11.331	0.272	0.001
6504	SLAMF1	signaling lymphocytic activation molecule family member 1	40.700	63.875	17.525	0.274	0.000
3805	KIR2DL4	killer cell immunoglobulin-like receptor, two domains, long cytoplasmic tail, 4	30.335	47.569	13.100	0.275	0.000

9580	SOX13	SRY (sex determining region Y)-box 13	25.152	39.441	10.862	0.275	0.000
387751	GVINP1	GTPase, very large interferon inducible pseudogene 1	50.983	79.883	22.082	0.276	0.000
255809	C19orf38	chromosome 19 open reading frame 38	217.978	341.364	94.593	0.277	0.000
9582	APOBEC3B	apolipoprotein B mRNA editing enzyme, catalytic polypeptide-like 3B	429.519	671.875	187.163	0.279	0.000
89858	SIGLEC12	sialic acid binding Ig-like lectin 12 (gene/pseudogene)	107.359	167.854	46.865	0.279	0.000
162466	PHOSPHO1	phosphatase, orphan 1	18.228	28.495	7.962	0.279	0.001
1E+08	NA	NA	17.129	26.770	7.488	0.280	0.003
23057	NMNAT2	nicotinamide nucleotide adenylyltransferase 2	77.367	120.843	33.891	0.280	0.000
3553	IL1B	interleukin 1, beta	208.608	324.960	92.256	0.284	0.000
25797	QPCT	glutaminyl-peptide cyclotransferase	28.567	44.497	12.636	0.284	0.000
27040	LAT	linker for activation of T cells	158.892	247.468	70.315	0.284	0.000
1101	CHAD	chondroadherin	18.840	29.318	8.361	0.285	0.001
57105	CYSLTR2	cysteinyl leukotriene receptor 2	63.651	98.979	28.323	0.286	0.000
283888	IL21R-AS1	IL21R antisense RNA 1	111.227	172.923	49.532	0.286	0.000
1588	CYP19A1	cytochrome P450, family 19, subfamily A, polypeptide 1	34.145	53.079	15.210	0.287	0.001
2634	GBP2	guanylate binding protein 2, interferon-inducible	654.367	1016.54	292.193	0.287	0.000
29950	SERTAD1	SERTA domain containing 1	55.446	86.132	24.760	0.287	0.000
3674	ITGA2B	integrin, alpha 2b (platelet glycoprotein IIb of IIb/IIIa complex, antigen CD41)	119.774	185.946	53.601	0.288	0.000
1116	CHI3L1	chitinase 3-like 1 (cartilage glycoprotein-39)	155.746	241.737	69.755	0.289	0.000
6508	SLC4A3	solute carrier family 4, anion exchanger, member 3	48.743	75.653	21.833	0.289	0.000
5724	PTAFR	platelet-activating factor receptor	278.644	432.131	125.157	0.290	0.000
911	CD1C	CD1c molecule	14.123	21.901	6.344	0.290	0.006
51738	GHRL	ghrelin/obestatin prepropeptide	26.256	40.715	11.796	0.290	0.000

146850	PIK3R6	phosphoinositide-3-kinase, regulatory subunit 6	51.765	80.222	23.308	0.291	0.000
1672	DEFB1	defensin, beta 1	29.786	46.142	13.431	0.291	0.000
5998	RGS3	regulator of G-protein signaling 3	28.491	44.133	12.850	0.291	0.000
200931	SLC51A	solute carrier family 51, alpha subunit	23.267	36.022	10.511	0.292	0.001
84446	BRSK1	BR serine/threonine kinase 1	32.764	50.703	14.825	0.292	0.000
360	AQP3	aquaporin 3 (Gill blood group)	17.044	26.360	7.729	0.293	0.006
27036	SIGLEC 7	sialic acid binding Ig-like lectin 7	69.863	108.045	31.681	0.293	0.000
5055	SERPIN B2	serpin peptidase inhibitor, clade B (ovalbumin), member 2	1239.75	1915.45	564.058	0.294	0.000
51267	CLEC1A	C-type lectin domain family 1, member A	13.064	20.179	5.950	0.295	0.010
9034	CCRL2	chemokine (C-C motif) receptor-like 2	20.238	31.255	9.221	0.295	0.002
6348	CCL3	chemokine (C-C motif) ligand 3	73.333	113.182	33.484	0.296	0.000
23710	GABAR APL1	GABA(A) receptor-associated protein like 1	136.420	210.172	62.667	0.298	0.000
978	CDA	cytidine deaminase	125.862	193.673	58.051	0.300	0.008
1953	MEGF6	multiple EGF-like-domains 6	25.268	38.877	11.658	0.300	0.001
54492	NEURL 1B	neuralized homolog 1B (Drosophila)	12.642	19.419	5.865	0.302	0.010
7052	TGM2	transglutaminase 2 (C polypeptide, protein-glutamine-gamma-glutamyltransferase)	21.395	32.857	9.933	0.302	0.001
5376	PMP22	peripheral myelin protein 22	121.033	185.867	56.200	0.302	0.000
3684	ITGAM	integrin, alpha M (complement component 3 receptor 3 subunit)	2092.63	3212.11	973.153	0.303	0.000
3628	INPP1	inositol polyphosphate-1-phosphatase	13.843	21.235	6.450	0.304	0.009
1E+08	NA	NA	79.290	121.576	37.003	0.304	0.001
11142	PKIG	protein kinase (cAMP-dependent, catalytic) inhibitor gamma	41.144	63.076	19.211	0.305	0.000
5920	RARRE S3	retinoic acid receptor responder (tazarotene induced) 3	19.818	30.368	9.269	0.305	0.001
1E+08	NA	NA	17.783	27.239	8.328	0.306	0.005

3809	KIR2DS4	killer cell immunoglobulin-like receptor, two domains, short cytoplasmic tail, 4	15.379	23.553	7.206	0.306	0.007
55803	ADAP2	ArfGAP with dual PH domains 2	102.736	157.333	48.139	0.306	0.000
8778	SIGLEC5	sialic acid binding Ig-like lectin 5	113.406	173.328	53.484	0.309	0.000
3575	IL7R	interleukin 7 receptor	2285.62	3491.82	1079.42	0.309	0.000
1E+08	LOC100506328	uncharacterized LOC100506328	16.162	24.676	7.648	0.310	0.004
51294	PCDH12	protocadherin 12	64.341	98.196	30.485	0.310	0.000
7022	TFAP2C	transcription factor AP-2 gamma (activating enhancer binding protein 2 gamma)	60.794	92.781	28.808	0.310	0.000
353514	LILRA5	leukocyte immunoglobulin-like receptor, subfamily A (with TM domain), member 5	464.947	709.182	220.711	0.311	0.000
80833	APOL3	apolipoprotein L, 3	50.785	77.319	24.251	0.314	0.000
23208	SYT11	synaptotagmin XI	355.270	540.740	169.799	0.314	0.000
5362	PLXNA2	plexin A2	99.487	151.327	47.647	0.315	0.000
1236	CCR7	chemokine (C-C motif) receptor 7	18.562	28.229	8.896	0.315	0.005
6279	S100A8	S100 calcium binding protein A8	8706.49	13231	4182.09	0.316	0.000
11025	LILRB3	leukocyte immunoglobulin-like receptor, subfamily B (with TM and ITIM domains), member 3	522.165	792.960	251.370	0.317	0.000
81848	SPRY4	sprouty homolog 4 (Drosophila)	37.501	56.940	18.062	0.317	0.000
2232	FDXR	ferredoxin reductase	309.156	469.282	149.031	0.318	0.000
8460	TPST1	tyrosylprotein sulfotransferase 1	39.327	59.687	18.967	0.318	0.000
9750	FAM65B	family with sequence similarity 65, member B	650.884	987.751	314.017	0.318	0.000
199675	C19orf59	chromosome 19 open reading frame 59	2200.32	3336.17	1064.47	0.319	0.000
6590	SLPI	secretory leukocyte peptidase inhibitor	48.746	73.909	23.582	0.319	0.000
144501	KRT80	keratin 80	102.012	154.565	49.459	0.320	0.000
116443	GRIN3A	glutamate receptor, ionotropic, N-methyl-D-aspartate 3A	107.397	162.580	52.213	0.321	0.000
56833	SLAMF8	SLAM family member 8	17.795	26.931	8.660	0.322	0.004
1E+08	NA	NA	21.722	32.871	10.574	0.322	0.002
57648	KIAA1522	KIAA1522	37.727	57.072	18.382	0.322	0.000

3097	HIVEP2	human immunodeficiency virus type I enhancer binding protein 2	24.582	37.182	11.982	0.322	0.001
933	CD22	CD22 molecule	24.968	37.753	12.183	0.323	0.002
84981	MIR22HG	MIR22 host gene (non-protein coding)	88.166	133.211	43.121	0.324	0.000
255031	FLJ35390	uncharacterized LOC255031	16.668	25.179	8.157	0.324	0.006
2268	FGR	Gardner-Rasheed feline sarcoma viral (v-fgr) oncogene homolog	1212.78	1831.40	594.158	0.324	0.000
79605	PGBD5	piggyBac transposable element derived 5	16.709	25.230	8.188	0.325	0.004
2015	EMR1	egf-like module containing, mucin-like, hormone receptor-like 1	161.797	244.218	79.377	0.325	0.000
57447	NDRG2	NDRG family member 2	62.421	94.153	30.689	0.326	0.000
10769	PLK2	polo-like kinase 2	1291.69	1948.14	635.246	0.326	0.000
55062	WIPI1	WD repeat domain, phosphoinositide interacting 1	155.320	234.088	76.551	0.327	0.000
23363	OBSL1	obscurin-like 1	193.822	291.920	95.725	0.328	0.001
165140	OXER1	oxoeicosanoid (OXE) receptor 1	56.230	84.681	27.779	0.328	0.000
2793	GNGT2	guanine nucleotide binding protein (G protein), gamma transducing activity polypeptide 2	60.828	91.560	30.095	0.329	0.000
5004	ORM1	orosomucoid 1	53.191	80.045	26.336	0.329	0.011
642402	LOC642402	golgin A6 family, member A pseudogene	41.995	63.131	20.860	0.330	0.003
27180	SIGLEC9	sialic acid binding Ig-like lectin 9	74.724	112.286	37.162	0.331	0.000
1958	EGR1	early growth response 1	110.428	165.908	54.948	0.331	0.000
9398	CD101	CD101 molecule	334.533	502.532	166.533	0.331	0.000
3914	LAMB3	laminin, beta 3	172.861	259.558	86.163	0.332	0.000
8676	STX11	syntaxin 11	87.097	130.766	43.427	0.332	0.000
1114	CHGB	chromogranin B (secretogranin 1)	20.867	31.312	10.422	0.333	0.004
84964	ALKBH6	alkB, alkylation repair homolog 6 (E. coli)	222.201	333.361	111.041	0.333	0.001
8870	IER3	immediate early response 3	46.570	69.860	23.280	0.333	0.000
1E+08	SIGLEC14	sialic acid binding Ig-like lectin 14	228.714	342.761	114.667	0.335	0.000
729574	LOC729574	UPF0627 protein ENSP00000341061/ENSP00000339743	17.839	26.710	8.968	0.336	0.008
7378	UPP1	uridine phosphorylase 1	81.226	121.544	40.908	0.337	0.000

55423	SIRPG	signal-regulatory protein gamma	73.693	110.153	37.233	0.338	0.000
1E+08	APOBEC3A_B	APOBEC3A and APOBEC3B deletion hybrid	54.404	81.315	27.494	0.338	0.000
56944	OLFML3	olfactomedin-like 3	42.557	63.599	21.515	0.338	0.000
4359	MPZ	myelin protein zero	454.350	678.970	229.729	0.338	0.000
197358	NLRC3	NLR family, CARD domain containing 3	686.698	1025.88	347.517	0.339	0.000
4327	MMP19	matrix metallopeptidase 19	107.433	160.477	54.390	0.339	0.000
27113	BBC3	BCL2 binding component 3	208.765	311.831	105.698	0.339	0.000
5732	PTGER2	prostaglandin E receptor 2 (subtype EP2), 53kDa	45.662	68.167	23.157	0.340	0.000
1053	CEBPE	CCAAT/enhancer binding protein (C/EBP), epsilon	77.937	116.318	39.556	0.340	0.000
4054	LTBP3	latent transforming growth factor beta binding protein 3	32.656	48.664	16.648	0.342	0.002
11178	LZTS1	leucine zipper, putative tumor suppressor 1	25.121	37.433	12.808	0.342	0.002
4035	LRP1	low density lipoprotein receptor-related protein 1	1559.74	2323.85	795.639	0.342	0.000
113675	SDSL	serine dehydratase-like	69.061	102.875	35.246	0.343	0.000
84286	TMEM175	transmembrane protein 175	76.241	113.468	39.015	0.344	0.003
167555	FAM151B	family with sequence similarity 151, member B	25.863	38.469	13.257	0.345	0.002
51311	TLR8	toll-like receptor 8	231.850	344.767	118.934	0.345	0.000
3732	CD82	CD82 molecule	726.297	1079.84	372.748	0.345	0.000
10347	ABCA7	ATP-binding cassette, sub-family A (ABC1), member 7	355.385	528.375	182.395	0.345	0.003
1880	GPR183	G protein-coupled receptor 183	888.057	1320.09	456.020	0.345	0.000
644165	BCRP3	breakpoint cluster region pseudogene 3	46.114	68.508	23.720	0.346	0.006
3561	IL2RG	interleukin 2 receptor, gamma	122.845	182.480	63.211	0.346	0.000
115817	DHRS1	dehydrogenase/reductase (SDR family) member 1	148.271	220.182	76.359	0.347	0.000
196883	ADCY4	adenylate cyclase 4	32.424	48.120	16.727	0.348	0.001
1E+08	ITGB2-AS1	ITGB2 antisense RNA 1	135.939	201.718	70.161	0.348	0.000
5553	PRG2	proteoglycan 2, bone marrow (natural killer cell activator, eosinophil granule major basic protein)	20.101	29.786	10.417	0.350	0.004

6349	CCL3L1	chemokine (C-C motif) ligand 3-like 1	136.325	201.715	70.935	0.352	0.000
83872	HMCN1	hemicentin 1	119.080	176.036	62.125	0.353	0.000
414062	CCL3L3	chemokine (C-C motif) ligand 3-like 3	135.799	200.663	70.935	0.354	0.000
3706	ITPKA	inositol-trisphosphate 3-kinase A	28.538	42.164	14.913	0.354	0.001
10871	CD300C	CD300c molecule	133.093	196.436	69.750	0.355	0.000
374403	TBC1D10C	TBC1 domain family, member 10C	53.969	79.636	28.302	0.355	0.002
122402	TDRD9	tudor domain containing 9	544.865	803.888	285.841	0.356	0.000
6347	CCL2	chemokine (C-C motif) ligand 2	377.914	557.535	198.293	0.356	0.006
3198	HOXA1	homeobox A1	55.670	82.089	29.252	0.356	0.000
646799	ZAR1L	zygote arrest 1-like	23.503	34.634	12.372	0.357	0.004
285848	PNPLA1	patatin-like phospholipase domain containing 1	60.365	88.790	31.939	0.360	0.000
419	ART3	ADP-ribosyltransferase 3	429.243	631.188	227.298	0.360	0.000
6817	SULT1A1	sulfotransferase family, cytosolic, 1A, phenol-preferring, member 1	139.685	205.380	73.991	0.360	0.009
54210	TREM1	triggering receptor expressed on myeloid cells 1	509.058	748.024	270.093	0.361	0.000
146547	PRSS36	protease, serine, 36	26.727	39.248	14.206	0.362	0.002
51716	CES1P1	carboxylesterase 1 pseudogene 1	1298.78	1905.59	691.968	0.363	0.000
1379	CR1L	complement component (3b/4b) receptor 1-like	53.280	78.142	28.418	0.364	0.000
4811	NID1	nidogen 1	126.745	185.875	67.615	0.364	0.000
5265	SERPINA1	serpin peptidase inhibitor, clade A (alpha-1 antiproteinase, antitrypsin), member 1	223.518	327.594	119.442	0.365	0.000
64174	DPEP2	dipeptidase 2	49.202	72.105	26.300	0.365	0.000
4900	NRGN	neurogranin (protein kinase C substrate, RC3)	323.549	474.123	172.975	0.365	0.010
23150	FRMD4B	FERM domain containing 4B	35.216	51.579	18.852	0.366	0.001
3120	HLA-DQB2	major histocompatibility complex, class II, DQ beta 2	65.939	96.399	35.478	0.368	0.000
3123	HLA-DRB1	major histocompatibility complex, class II, DR beta 1	307.246	448.639	165.852	0.370	0.000
1515	CTSL2	cathepsin L2	70.667	103.174	38.160	0.370	0.000
1E+08	APOBEC3B-AS1	APOBEC3B antisense RNA 1	47.370	69.159	25.581	0.370	0.000

3606	IL18	interleukin 18 (interferon-gamma-inducing factor)	408.485	596.156	220.814	0.370	0.000
2635	GBP3	guanylate binding protein 3	246.646	359.894	133.399	0.371	0.000
347735	SERINC2	serine incorporator 2	589.999	860.880	319.118	0.371	0.000
399694	SHC4	SHC (Src homology 2 domain containing) family, member 4	21.476	31.324	11.628	0.371	0.009
80705	TSGA10	testis specific, 10	22.167	32.332	12.002	0.371	0.006
4640	MYO1A	myosin IA	21.995	32.072	11.918	0.372	0.005
3119	HLA-DQB1	major histocompatibility complex, class II, DQ beta 1	387.094	564.165	210.022	0.372	0.000
7039	TGFA	transforming growth factor, alpha	44.400	64.697	24.103	0.373	0.011
6714	SRC	v-src sarcoma (Schmidt-Ruppin A-2) viral oncogene homolog (avian)	166.135	241.960	90.309	0.373	0.000
84627	ZNF469	zinc finger protein 469	75.886	110.520	41.253	0.373	0.000
84795	PYROXD2	pyridine nucleotide-disulphide oxidoreductase domain 2	49.573	72.196	26.949	0.373	0.000
6280	S100A9	S100 calcium binding protein A9	36180.6	52690	19670.8	0.373	0.003
3695	ITGB7	integrin, beta 7	1057.96	1539.09	576.838	0.375	0.000
1366	CLDN7	claudin 7	53.214	77.411	29.016	0.375	0.001
116844	LRG1	leucine-rich alpha-2-glycoprotein 1	352.226	512.282	192.169	0.375	0.000
724033	MIR663A	microRNA 663a	537.673	781.867	293.479	0.375	0.009
56666	PANX2	pannexin 2	22.603	32.856	12.349	0.376	0.006
433	ASGR2	asialoglycoprotein receptor 2	71.792	104.352	39.233	0.376	0.000
246329	STAC3	SH3 and cysteine rich domain 3	713.531	1036.73	390.328	0.376	0.000
54535	CCHCR1	coiled-coil alpha-helical rod protein 1	197.395	286.721	108.069	0.377	0.002
23584	VSIG2	V-set and immunoglobulin domain containing 2	69.394	100.603	38.184	0.380	0.000
25822	DNAJB5	DnaJ (Hsp40) homolog, subfamily B, member 5	21.569	31.267	11.871	0.380	0.009
401944	LDLRAD2	low density lipoprotein receptor class A domain containing 2	90.208	130.699	49.717	0.380	0.000
4688	NCF2	neutrophil cytosolic factor 2	1875.46	2717.03	1033.89	0.381	0.000
3959	LGALS3BP	lectin, galactoside-binding, soluble, 3 binding protein	364.162	527.324	201.000	0.381	0.000

2354	FOSB	FBJ murine osteosarcoma viral oncogene homolog B	48.403	70.071	26.734	0.382	0.000
55337	C19orf66	chromosome 19 open reading frame 66	87.459	126.536	48.382	0.382	0.000
728113	ANXA8L1	annexin A8-like 1	279.297	403.650	154.943	0.384	0.000
9537	TP53I11	tumor protein p53 inducible protein 11	564.552	815.253	313.851	0.385	0.000
57509	MTUS1	microtubule associated tumor suppressor 1	86.803	125.318	48.287	0.385	0.005
5005	ORM2	orosomucoid 2	31.866	45.982	17.749	0.386	0.001
54874	FNBP1L	formin binding protein 1-like	41.168	59.396	22.941	0.386	0.001
278	AMY1C	amylase, alpha 1C (salivary)	1047.80	1511.54	584.064	0.386	0.000
710	SERPING1	serpin peptidase inhibitor, clade G (C1 inhibitor), member 1	42.807	61.736	23.878	0.387	0.001
277	AMY1B	amylase, alpha 1B (salivary)	1046.81	1509.55	584.064	0.387	0.000
148523	C1orf51	chromosome 1 open reading frame 51	37.842	54.529	21.154	0.388	0.001
276	AMY1A	amylase, alpha 1A (salivary)	1050.13	1512.41	587.849	0.389	0.000
653145	ANXA8	annexin A8	597.069	859.678	334.460	0.389	0.000
150365	MEI1	meiosis inhibitor 1	77.641	111.734	43.548	0.390	0.000
2651	GCNT2	glucosaminyl (N-acetyl) transferase 2, I-branching enzyme (I blood group)	25.148	36.173	14.122	0.390	0.009
55359	STYK1	serine/threonine/tyrosine kinase 1	41.527	59.708	23.346	0.391	0.008
51733	UPB1	ureidopropionase, beta	99.703	143.214	56.193	0.392	0.000
1E+08	NA	NA	33.956	48.758	19.154	0.393	0.002
5768	QSOX1	quiescin Q6 sulfhydryl oxidase 1	2178.96	3128.35	1229.57	0.393	0.000
1509	CTSD	cathepsin D	1230.10	1765.81	694.391	0.393	0.005
285084	LOC285084	uncharacterized LOC285084	776.211	1114.04	438.385	0.394	0.000
10626	TRIM16	tripartite motif containing 16	604.130	865.761	342.500	0.396	0.000
4485	MST1	macrophage stimulating 1 (hepatocyte growth factor-like)	164.089	235.133	93.045	0.396	0.000
80832	APOL4	apolipoprotein L, 4	1430.78	2049.94	811.620	0.396	0.000
9064	MAP3K6	mitogen-activated protein kinase kinase kinase 6	509.224	729.581	288.867	0.396	0.000
2217	FCGRT	Fc fragment of IgG, receptor, transporter, alpha	724.809	1038.38	411.238	0.396	0.000

11223	MST1L	macrophage stimulating 1-like	57.352	82.152	32.552	0.396	0.000
57153	SLC44A2	solute carrier family 44, member 2	312.132	447.049	177.215	0.396	0.000
80150	ASRGL1	asparaginase like 1	86.956	124.518	49.393	0.397	0.000
8651	SOCS1	suppressor of cytokine signaling 1	90.656	129.799	51.512	0.397	0.000
25841	ABTB2	ankyrin repeat and BTB (POZ) domain containing 2	424.470	607.446	241.495	0.398	0.000
285852	TREML4	triggering receptor expressed on myeloid cells-like 4	21.089	30.137	12.041	0.400	0.010
6303	SAT1	spermidine/spermine N1-acetyltransferase 1	1945.12	2778.63	1111.61	0.400	0.000
5272	SERPINB9	serpin peptidase inhibitor, clade B (ovalbumin), member 9	345.143	492.774	197.512	0.401	0.000
9764	KIAA0513	KIAA0513	174.705	249.221	100.189	0.402	0.000
57413	NA	NA	55.584	79.254	31.914	0.403	0.000
57175	CORO1B	coronin, actin binding protein, 1B	310.316	442.078	178.554	0.404	0.000
11209	MST1P2	macrophage stimulating 1 (hepatocyte growth factor-like) pseudogene 2	76.515	108.963	44.066	0.404	0.000
2906	GRIN2D	glutamate receptor, ionotropic, N-methyl D-aspartate 2D	99.718	142.004	57.432	0.404	0.000
151534	LBX2-AS1	LBX2 antisense RNA 1	31.111	44.280	17.942	0.405	0.004
64581	CLEC7A	C-type lectin domain family 7, member A	185.998	264.695	107.302	0.405	0.005
25959	KANK2	KN motif and ankyrin repeat domains 2	399.102	567.602	230.602	0.406	0.000
3579	CXCR2	chemokine (C-X-C motif) receptor 2	599.094	851.906	346.283	0.406	0.000
63874	ABHD4	abhydrolase domain containing 4	40.326	57.298	23.353	0.408	0.002
677	ZFP36L1	ZFP36 ring finger protein-like 1	63.437	90.119	36.755	0.408	0.000
6282	S100A11	S100 calcium binding protein A11	504.194	716.184	292.204	0.408	0.002
83959	SLC4A11	solute carrier family 4, sodium borate transporter, member 11	38.007	53.973	22.040	0.408	0.001
3594	IL12RB1	interleukin 12 receptor, beta 1	718.357	1019.73	416.979	0.409	0.000
5800	PTPRO	protein tyrosine phosphatase, receptor type, O	1085.81	1540.65	630.958	0.410	0.000

79865	TREML2	triggering receptor expressed on myeloid cells-like 2	498.534	707.340	289.728	0.410	0.000
346389	MACC1	metastasis associated in colon cancer 1	58.946	83.597	34.296	0.410	0.000
2811	GP1BA	glycoprotein Ib (platelet), alpha polypeptide	23.605	33.464	13.746	0.411	0.008
56548	CHST7	carbohydrate (N-acetylglucosamine 6-O) sulfotransferase 7	27.341	38.757	15.925	0.411	0.008
10365	KLF2	Kruppel-like factor 2 (lung)	23.879	33.848	13.909	0.411	0.008
3958	LGALS3	lectin, galactoside-binding, soluble, 3	61.276	86.795	35.757	0.412	0.000
10970	CKAP4	cytoskeleton-associated protein 4	2754.7	3899.56	1609.84	0.413	0.000
7292	TNFSF4	tumor necrosis factor (ligand) superfamily, member 4	36.458	51.567	21.349	0.414	0.004
162394	SLFN5	schlafen family member 5	64.950	91.864	38.036	0.414	0.000
79930	DOK3	docking protein 3	202.264	286.060	118.467	0.414	0.000
6036	RNASE2	ribonuclease, RNase A family, 2 (liver, eosinophil-derived neurotoxin)	1796.93	2540.84	1053.02	0.414	0.000
83666	PARP9	poly (ADP-ribose) polymerase family, member 9	565.775	799.944	331.606	0.415	0.000
386627	FLJ38109	uncharacterized LOC386627	37.769	53.395	22.143	0.415	0.002
64410	KLHL25	kelch-like family member 25	39.566	55.892	23.240	0.416	0.002
375033	PEAR1	platelet endothelial aggregation receptor 1	52.533	74.145	30.922	0.417	0.001
8900	CCNA1	cyclin A1	451.506	637.218	265.794	0.417	0.000
84868	HAVCR2	hepatitis A virus cellular receptor 2	366.897	517.400	216.395	0.418	0.000
8792	TNFRSF11A	tumor necrosis factor receptor superfamily, member 11a, NFKB activator	23.922	33.731	14.113	0.418	0.012
51268	PIPOX	pipecolic acid oxidase	108.688	153.147	64.229	0.419	0.000
2687	GGT5	gamma-glutamyltransferase 5	225.227	317.019	133.435	0.421	0.001
64866	CDCP1	CUB domain containing protein 1	27.971	39.368	16.574	0.421	0.009
3306	HSPA2	heat shock 70kDa protein 2	130.057	183.041	77.074	0.421	0.000
10068	IL18BP	interleukin 18 binding protein	144.405	203.132	85.677	0.422	0.009
114787	GPRIN1	G protein regulated inducer of neurite	56.238	79.098	33.378	0.422	0.000

		outgrowth 1					
374393	FAM111B	family with sequence similarity 111, member B	65.316	91.839	38.793	0.422	0.000
3433	IFIT2	interferon-induced protein with tetratricopeptide repeats 2	51.637	72.596	30.678	0.423	0.008
57121	LPAR5	lysophosphatidic acid receptor 5	34.922	49.061	20.784	0.424	0.003
29965	CDIP1	cell death-inducing p53 target 1	107.878	151.509	64.247	0.424	0.000
115677	NOSTRIN	nitric oxide synthase trafficker	55.394	77.797	32.991	0.424	0.000
3576	IL8	interleukin 8	1664.49	2335.97	993.009	0.425	0.001
57520	HECW2	HECT, C2 and WW domain containing E3 ubiquitin protein ligase 2	46.566	65.305	27.827	0.426	0.002
94120	SYTL3	synaptotagmin-like 3	279.685	392.172	167.197	0.426	0.000
140766	ADAMTS14	ADAM metallopeptidase with thrombospondin type 1 motif, 14	30.324	42.518	18.131	0.426	0.005
5129	CDK18	cyclin-dependent kinase 18	25.998	36.450	15.546	0.427	0.007
308	ANXA5	annexin A5	1017.37	1426.35	608.390	0.427	0.000
151056	PLB1	phospholipase B1	167.795	235.167	100.422	0.427	0.000
3856	KRT8	keratin 8	44.254	62.006	26.502	0.427	0.002
5159	PDGFRB	platelet-derived growth factor receptor, beta polypeptide	26.605	37.265	15.945	0.428	0.007
5794	PTPRH	protein tyrosine phosphatase, receptor type, H	56.470	79.077	33.863	0.428	0.001
94241	TP53INP1	tumor protein p53 inducible nuclear protein 1	1330.69	1863.37	798.011	0.428	0.006
9540	TP53I3	tumor protein p53 inducible protein 3	89.893	125.865	53.920	0.428	0.000
55911	APOBR	apolipoprotein B receptor	587.730	822.839	352.621	0.429	0.005
9746	CLSTN3	calsyntenin 3	733.985	1027.41	440.557	0.429	0.000
79659	DYNC2H1	dynein, cytoplasmic 2, heavy chain 1	44.928	62.863	26.993	0.429	0.002
26020	LRP10	low density lipoprotein receptor-related protein 10	776.362	1086.21	466.513	0.429	0.000
51313	FAM198B	family with sequence similarity 198, member B	160.330	224.305	96.355	0.430	0.000
4343	MOV10	Mov10, Moloney leukemia virus 10, homolog (mouse)	501.236	700.950	301.522	0.430	0.000
64108	RTP4	receptor (chemosensory) transporter protein 4	77.726	108.678	46.774	0.430	0.000

79899	PRR5L	proline rich 5 like	111.499	155.859	67.140	0.431	0.000
9050	PSTPIP2	proline-serine-threonine phosphatase interacting protein 2	271.488	379.415	163.561	0.431	0.000
55711	FAR2	fatty acyl CoA reductase 2	159.384	222.651	96.117	0.432	0.000
144097	C11orf84	chromosome 11 open reading frame 84	237.404	331.477	143.331	0.432	0.000
4241	MFI2	antigen p97 (melanoma associated) identified by monoclonal antibodies 133.2 and 96.5	239.883	334.895	144.870	0.433	0.007
3128	HLA-DRB6	major histocompatibility complex, class II, DR beta 6 (pseudogene)	62.327	86.975	37.680	0.433	0.009
284124	FLJ36000	uncharacterized FLJ36000	956.629	1333.61	579.645	0.435	0.000
55723	ASF1B	ASF1 anti-silencing function 1 homolog B (S. cerevisiae)	1782.51	2484.58	1080.44	0.435	0.000
290	ANPEP	alanyl (membrane) aminopeptidase	2999.86	4180.54	1819.19	0.435	0.000
85474	LBX2	ladybird homeobox 2	40.024	55.744	24.305	0.436	0.003
1152	CKB	creatine kinase, brain	33.253	46.282	20.223	0.437	0.008
7832	BTG2	BTG family, member 2	1124.95	1565.67	684.229	0.437	0.000
113452	TMEM54	transmembrane protein 54	55.707	77.525	33.889	0.437	0.001
401331	RASA4CP	RAS p21 protein activator 4C, pseudogene	58.464	81.357	35.570	0.437	0.001
11346	SYNPO	synaptopodin	51.905	72.192	31.619	0.438	0.004
1066	CES1	carboxylesterase 1	6959.77	9677.47	4242.07	0.438	0.000
3385	ICAM3	intercellular adhesion molecule 3	697.930	970.458	425.402	0.438	0.005
3300	DNAJB2	DnaJ (Hsp40) homolog, subfamily B, member 2	146.930	204.256	89.604	0.439	0.001
5360	PLTP	phospholipid transfer protein	85.427	118.734	52.120	0.439	0.008
474344	GIMAP6	GTPase, IMAP family member 6	392.454	545.291	239.617	0.439	0.000
51816	CECR1	cat eye syndrome chromosome region, candidate 1	220.770	306.713	134.828	0.440	0.000
10924	SMPDL3A	sphingomyelin phosphodiesterase, acid-like 3A	237.380	329.684	145.077	0.440	0.000
83861	RSPH3	radial spoke 3 homolog (Chlamydomonas)	114.922	159.589	70.255	0.440	0.000
56265	CPXM1	carboxypeptidase X (M14 family), member 1	415.979	577.087	254.871	0.442	0.000
64333	ARHGA	Rho GTPase activating	1195.84	1658.61	733.069	0.442	0.000

	P9	protein 9					
5742	PTGS1	prostaglandin-endoperoxide synthase 1 (prostaglandin G/H synthase and cyclooxygenase)	92.582	128.382	56.782	0.442	0.000
85441	HELZ2	helicase with zinc finger 2, transcriptional coactivator	119.062	165.069	73.055	0.443	0.000
165186	FAM179A	family with sequence similarity 179, member A	43.159	59.836	26.482	0.443	0.002
84803	AGPAT9	1-acylglycerol-3-phosphate O-acyltransferase 9	207.284	287.362	127.206	0.443	0.007
3566	IL4R	interleukin 4 receptor	646.401	895.922	396.880	0.443	0.000
942	CD86	CD86 molecule	569.942	789.492	350.392	0.444	0.003
170371	C10orf128	chromosome 10 open reading frame 128	184.924	256.047	113.802	0.444	0.000
5600	MAPK11	mitogen-activated protein kinase 11	38.181	52.828	23.534	0.445	0.003
967	CD63	CD63 molecule	850.626	1176.53	524.720	0.446	0.005
116729	PPP1R27	protein phosphatase 1, regulatory subunit 27	43.011	59.487	26.534	0.446	0.002
6609	SMPD1	sphingomyelin phosphodiesterase 1, acid lysosomal	141.327	195.409	87.244	0.446	0.004
3559	IL2RA	interleukin 2 receptor, alpha	288.400	398.746	178.055	0.447	0.000
220108	FAM124A	family with sequence similarity 124A	149.797	207.091	92.503	0.447	0.000
3242	HPD	4-hydroxyphenylpyruvate dioxygenase	146.284	202.193	90.374	0.447	0.001
2034	EPAS1	endothelial PAS domain protein 1	177.078	244.583	109.573	0.448	0.000
79630	C1orf54	chromosome 1 open reading frame 54	491.734	679.173	304.295	0.448	0.002
59342	SCPEP1	serine carboxypeptidase 1	974.806	1344.37	605.242	0.450	0.000
23670	TMEM2	transmembrane protein 2	161.219	222.295	100.143	0.450	0.000
2319	FLOT2	flotillin 2	1613.38	2224.27	1002.49	0.451	0.001
3816	KLK1	kallikrein 1	62.208	85.746	38.671	0.451	0.001
3797	KIF3C	kinesin family member 3C	397.831	548.135	247.527	0.452	0.000
9114	ATP6V0D1	ATPase, H+ transporting, lysosomal 38kDa, V0 subunit d1	664.279	915.064	413.494	0.452	0.002
140564	APOBEC3D	apolipoprotein B mRNA editing enzyme, catalytic polypeptide-like 3D	155.347	213.963	96.731	0.452	0.000

5337	PLD1	phospholipase D1, phosphatidylcholine-specific	572.798	788.812	356.784	0.452	0.000
5803	PTPRZ1	protein tyrosine phosphatase, receptor-type, Z polypeptide 1	346.439	476.990	215.888	0.453	0.000
29785	CYP2S1	cytochrome P450, family 2, subfamily S, polypeptide 1	144.125	198.413	89.837	0.453	0.000
23547	LILRA4	leukocyte immunoglobulin-like receptor, subfamily A (with TM domain), member 4	39.969	54.968	24.971	0.454	0.004
10133	OPTN	optineurin	159.781	219.705	99.857	0.455	0.001
32	ACACB	acetyl-CoA carboxylase beta	242.557	333.513	151.602	0.455	0.000
150221	RIMBP3C	RIMS binding protein 3C	158.867	218.392	99.343	0.455	0.004
440804	RIMBP3B	RIMS binding protein 3B	158.867	218.392	99.343	0.455	0.004
3310	HSPA6	heat shock 70kDa protein 6 (HSP70B')	84.093	115.581	52.605	0.455	0.000
161582	DYX1C1	dyslexia susceptibility 1 candidate 1	41.798	57.377	26.219	0.457	0.008
94097	SFXN5	sideroflexin 5	44.947	61.671	28.222	0.458	0.002
121512	FGD4	FYVE, RhoGEF and PH domain containing 4	708.928	972.635	445.222	0.458	0.002
129607	CMPK2	cytidine monophosphate (UMP-CMP) kinase 2, mitochondrial	118.788	162.963	74.612	0.458	0.000
1396	CRIP1	cysteine-rich protein 1 (intestinal)	163.024	223.593	102.455	0.458	0.001
8309	ACOX2	acyl-CoA oxidase 2, branched chain	82.270	112.784	51.755	0.459	0.000
23780	APOL2	apolipoprotein L, 2	486.879	667.277	306.481	0.459	0.000
10610	ST6GALNAC2	ST6 (alpha-N-acetyl-neuraminyl-2,3-beta-galactosyl-1,3)-N-acetylgalactosaminide alpha-2,6-sialyltransferase 2	44.727	61.281	28.173	0.460	0.003
1E+08	LOC100129083	uncharacterized LOC100129083	70.268	96.242	44.294	0.460	0.010
7185	TRAF1	TNF receptor-associated factor 1	121.997	166.882	77.111	0.462	0.000
352954	GATS	GATS, stromal antigen 3 opposite strand	58.824	80.436	37.213	0.463	0.001
154881	KCTD7	potassium channel tetramerisation domain containing 7	121.393	165.889	76.896	0.464	0.000

339541	C1orf228	chromosome 1 open reading frame 228	133.912	182.947	84.876	0.464	0.000
83853	ROPN1L	rhophilin associated tail protein 1-like	77.285	105.557	49.013	0.464	0.001
7060	THBS4	thrombospondin 4	230.908	315.309	146.506	0.465	0.000
445347	TARP	TCR gamma alternate reading frame protein	2059.68	2811.81	1307.55	0.465	0.000
9938	ARHGAP25	Rho GTPase activating protein 25	806.707	1101.21	512.200	0.465	0.000
10745	PHTF1	putative homeodomain transcription factor 1	526.295	718.382	334.209	0.465	0.000
10437	IFI30	interferon, gamma-inducible protein 30	261.975	357.570	166.379	0.465	0.000
3290	HSD11B1	hydroxysteroid (11-beta) dehydrogenase 1	477.055	651.029	303.082	0.466	0.000
1E+08	LRRC37A8P	leucine rich repeat containing 37, member A8, pseudogene	55.919	76.304	35.534	0.466	0.002
9600	PITPNM1	phosphatidylinositol transfer protein, membrane-associated 1	298.533	407.305	189.761	0.466	0.001
124599	CD300LB	CD300 molecule-like family member b	86.804	118.348	55.259	0.467	0.001
4608	MYBPH	myosin binding protein H	561.088	764.951	357.225	0.467	0.005
85376	RIMBP3	RIMS binding protein 3	82.733	112.785	52.681	0.467	0.010
10044	SH2D3C	SH2 domain containing 3C	292.041	398.104	185.978	0.467	0.000
303	ANXA2P1	annexin A2 pseudogene 1	162.127	220.994	103.260	0.467	0.007
404093	CUEDC1	CUE domain containing 1	159.702	217.666	101.739	0.467	0.000
91544	UBXN11	UBX domain protein 11	856.760	1166.86	546.661	0.468	0.001
400709	SIGLEC16	sialic acid binding Ig-like lectin 16 (gene/pseudogene)	88.225	120.099	56.350	0.469	0.000
27350	APOBEC3C	apolipoprotein B mRNA editing enzyme, catalytic polypeptide-like 3C	951.302	1294.94	607.664	0.469	0.000
3749	KCNC4	potassium voltage-gated channel, Shaw-related subfamily, member 4	61.287	83.401	39.174	0.470	0.002
90273	CEACAM21	carcinoembryonic antigen-related cell adhesion molecule 21	86.768	118.055	55.481	0.470	0.001
6385	SDC4	syndecan 4	84.882	115.489	54.276	0.470	0.000
79640	C22orf46	chromosome 22 open reading frame 46	351.816	478.523	225.109	0.470	0.005
2204	FCAR	Fc fragment of IgA,	284.708	387.197	182.219	0.471	0.000

		receptor for					
51744	CD244	CD244 molecule, natural killer cell receptor 2B4	81.999	111.508	52.491	0.471	0.001
10288	LILRB2	leukocyte immunoglobulin-like receptor, subfamily B (with TM and ITIM domains), member 2	881.094	1198.11	564.080	0.471	0.000
9826	ARHGEF11	Rho guanine nucleotide exchange factor (GEF) 11	156.737	213.065	100.408	0.471	0.000
5168	ENPP2	ectonucleotide pyrophosphatase/phosphodiesterase 2	410.223	557.508	262.937	0.472	0.000
1870	E2F2	E2F transcription factor 2	590.725	802.596	378.855	0.472	0.000
1601	DAB2	disabled homolog 2, mitogen-responsive phosphoprotein (Drosophila)	185.644	252.146	119.142	0.473	0.000
8741	TNFSF13	tumor necrosis factor (ligand) superfamily, member 13	375.131	509.169	241.093	0.474	0.001
353189	SLCO4C1	solute carrier organic anion transporter family, member 4C1	501.857	680.900	322.814	0.474	0.003
3339	HSPG2	heparan sulfate proteoglycan 2	427.127	579.027	275.227	0.475	0.000
5274	SERPINI1	serpin peptidase inhibitor, clade I (neuroserpin), member 1	45.874	62.165	29.583	0.476	0.004
2833	CXCR3	chemokine (C-X-C motif) receptor 3	156.944	212.677	101.210	0.476	0.000
9466	IL27RA	interleukin 27 receptor, alpha	112.690	152.701	72.679	0.476	0.010
2212	FCGR2A	Fc fragment of IgG, low affinity IIa, receptor (CD32)	4513.30	6115.67	2910.93	0.476	0.005
5871	MAP4K2	mitogen-activated protein kinase kinase kinase kinase 2	227.494	308.245	146.743	0.476	0.000
407977	TNFSF12-TNFSF13	TNFSF12-TNFSF13 readthrough	332.327	450.247	214.407	0.476	0.000
3321	IGSF3	immunoglobulin superfamily, member 3	209.307	283.263	135.350	0.478	0.000
6539	SLC6A12	solute carrier family 6 (neurotransmitter transporter, betaine/GABA), member 12	49.685	67.224	32.146	0.478	0.003
286	ANK1	ankyrin 1, erythrocytic	49.220	66.593	31.848	0.478	0.004

6688	SPI1	spleen focus forming virus (SFFV) proviral integration oncogene spi1	912.295	1234.04	590.554	0.479	0.011
80212	CCDC92	coiled-coil domain containing 92	48.234	65.234	31.234	0.479	0.006
6804	STX1A	syntaxin 1A (brain)	110.558	149.520	71.597	0.479	0.004
219285	SAMD9L	sterile alpha motif domain containing 9-like	730.108	987.340	472.877	0.479	0.001
837	CASP4	caspase 4, apoptosis-related cysteine peptidase	810.905	1096.19	525.618	0.479	0.000
37	ACADVL	acyl-CoA dehydrogenase, very long chain	4804.16	6494.26	3114.05	0.480	0.000
8972	MGAM	maltase-glucoamylase (alpha-glucosidase)	389.008	525.829	252.187	0.480	0.000
1378	CR1	complement component (3b/4b) receptor 1 (Knops blood group)	1412.37	1908.76	915.968	0.480	0.000
8497	PPFIA4	protein tyrosine phosphatase, receptor type, f polypeptide (PTPRF), interacting protein (liprin), alpha 4	283.362	382.868	183.856	0.480	0.000
2679	GGT3P	gamma-glutamyltransferase 3 pseudogene	120.809	163.218	78.400	0.480	0.006
9402	GRAP2	GRB2-related adaptor protein 2	81.657	110.315	52.999	0.480	0.001
64080	RBKS	ribokinase	94.257	127.337	61.177	0.480	0.001
4778	NFE2	nuclear factor (erythroid-derived 2), 45kDa	551.000	744.256	357.743	0.481	0.000
5212	VIT	vitrin	163.381	220.664	106.098	0.481	0.000
27154	BRPF3	bromodomain and PHD finger containing, 3	710.144	959.104	461.184	0.481	0.000
304	ANXA2P2	annexin A2 pseudogene 2	1825.24	2463.89	1186.58	0.482	0.000
10493	VAT1	vesicle amine transport protein 1 homolog (T. californica)	1837.52	2480.37	1194.67	0.482	0.000
145957	NRG4	neuregulin 4	204.862	276.458	133.267	0.482	0.001
467	ATF3	activating transcription factor 3	202.593	273.333	131.852	0.482	0.000
1606	DGKA	diacylglycerol kinase, alpha 80kDa	655.189	883.943	426.434	0.482	0.001
202	AIM1	absent in melanoma 1	1155.03	1557.97	752.080	0.483	0.000
1084	CEACAM3	carcinoembryonic antigen-related cell adhesion molecule 3	68.667	92.612	44.722	0.483	0.001
55367	PIDD	p53-induced death domain protein	408.058	549.916	266.200	0.484	0.003

60489	APOBEC3G	apolipoprotein B mRNA editing enzyme, catalytic polypeptide-like 3G	154.871	208.659	101.084	0.484	0.000
8061	FOSL1	FOS-like antigen 1	86.815	116.949	56.682	0.485	0.000
92154	MTSS1L	metastasis suppressor 1-like	62.492	84.168	40.817	0.485	0.011
23053	ZSWIM8	zinc finger, SWIM-type containing 8	671.462	903.883	439.040	0.486	0.001
8418	CMAHP	cytidine monophospho-N-acetylneuraminic acid hydroxylase, pseudogene	322.110	433.490	210.730	0.486	0.000
10039	PARP3	poly (ADP-ribose) polymerase family, member 3	149.736	201.498	97.973	0.486	0.000
2210	FCGR1B	Fc fragment of IgG, high affinity Ib, receptor (CD64)	907.713	1221.09	594.339	0.487	0.000
6352	CCL5	chemokine (C-C motif) ligand 5	631.318	849.096	413.541	0.487	0.000
1643	DDB2	damage-specific DNA binding protein 2, 48kDa	1324.61	1781.34	867.876	0.487	0.000
3311	HSPA7	heat shock 70kDa protein 7 (HSP70B)	105.018	141.102	68.934	0.489	0.000
133396	IL31RA	interleukin 31 receptor A	541.706	727.556	355.856	0.489	0.000
10326	SIRPB1	signal-regulatory protein beta 1	1644.26	2207.62	1080.91	0.490	0.000
94032	CAMK2N2	calcium/calmodulin-dependent protein kinase II inhibitor 2	40.477	54.340	26.613	0.490	0.008
120425	AMICA1	adhesion molecule, interacts with CXADR antigen 1	835.676	1121.51	549.843	0.490	0.000
9051	PSTPIP1	proline-serine-threonine phosphatase interacting protein 1	561.131	752.896	369.366	0.491	0.000
1E+08	FCGR1C	Fc fragment of IgG, high affinity Ic, receptor (CD64), pseudogene	890.373	1194.14	586.601	0.491	0.000
389792	IER5L	immediate early response 5-like	182.905	245.218	120.593	0.492	0.006
948	CD36	CD36 molecule (thrombospondin receptor)	3185.23	4269.44	2101.02	0.492	0.009
1E+08	IQCJ-SCHIP1	IQCJ-SCHIP1 readthrough	418.728	561.244	276.211	0.492	0.005
29970	SCHIP1	schwannomin interacting protein 1	421.969	565.538	278.401	0.492	0.005
6560	SLC12A4	solute carrier family 12 (potassium/chloride transporters), member 4	563.891	755.534	372.249	0.493	0.000
3092	HIP1	huntingtin interacting protein 1	2333.73	3126.28	1541.18	0.493	0.000

56935	C11orf75	chromosome 11 open reading frame 75	91.357	122.371	60.344	0.493	0.002
2841	GPR18	G protein-coupled receptor 18	217.871	291.796	143.946	0.493	0.000
92691	TMEM169	transmembrane protein 169	64.742	86.654	42.830	0.494	0.003
54507	ADAMTSL4	ADAMTS-like 4	440.310	589.172	291.448	0.495	0.000
79733	E2F8	E2F transcription factor 8	1145.29	1532.45	758.137	0.495	0.000
137835	TMEM71	transmembrane protein 71	182.691	244.411	120.970	0.495	0.000
6277	S100A6	S100 calcium binding protein A6	867.428	1160.01	574.846	0.496	0.000
3437	IFIT3	interferon-induced protein with tetratricopeptide repeats 3	113.985	152.381	75.589	0.496	0.000
84875	PARP10	poly (ADP-ribose) polymerase family, member 10	472.902	631.461	314.343	0.498	0.001
3687	ITGAX	integrin, alpha X (complement component 3 receptor 4 subunit)	720.073	961.030	479.116	0.499	0.000
10211	FLOT1	flotillin 1	579.336	772.915	385.757	0.499	0.000
89790	SIGLEC10	sialic acid binding Ig-like lectin 10	243.081	324.160	162.002	0.500	0.001
55008	HERC6	HECT and RLD domain containing E3 ubiquitin protein ligase family member 6	123.078	164.104	82.052	0.500	0.003
1E+08	NA	NA	55.321	36.846	73.796	2.003	0.006
51076	CUTC	cutC copper transporter homolog (E. coli)	1155.28	769.277	1541.28	2.004	0.000
65084	TMEM135	transmembrane protein 135	1479.94	984.217	1975.67	2.007	0.000
5831	PYCR1	pyrroline-5-carboxylate reductase 1	137.261	91.275	183.248	2.008	0.010
55172	DNAAF2	dynein, axonemal, assembly factor 2	493.953	328.393	659.512	2.008	0.000
153364	MBLAC2	metallo-beta-lactamase domain containing 2	407.201	270.670	543.731	2.009	0.000
2632	GBE1	glucan (1,4-alpha-), branching enzyme 1	3184.84	2116.81	4252.88	2.009	0.000
1E+08	LOC100190986	uncharacterized LOC100190986	933.875	620.609	1247.14	2.010	0.002
5935	RBM3	RNA binding motif (RNP1, RRM) protein 3	37705.3	25049.9	50360.7	2.010	0.000
57546	PDP2	pyruvate dehyrogenase phosphatase catalytic subunit 2	2034.48	1351.01	2717.96	2.012	0.000
5581	PRKCE	protein kinase C, epsilon	408.427	271.084	545.770	2.013	0.000

147727	ILF3-AS1	ILF3 antisense RNA 1 (head to head)	487.504	323.497	651.511	2.014	0.000
8204	NRIP1	nuclear receptor interacting protein 1	3151.11	2090.36	4211.86	2.015	0.000
80155	NAA15	N(alpha)-acetyltransferase 15, NatA auxiliary subunit	8048.42	5338.16	10758.7	2.015	0.000
196394	AMN1	antagonist of mitotic exit network 1 homolog (S. cerevisiae)	407.336	269.844	544.827	2.019	0.000
6641	SNTB1	syntrophin, beta 1 (dystrophin-associated protein A1, 59kDa, basic component 1)	1484.22	983.042	1985.39	2.020	0.000
23160	WDR43	WD repeat domain 43	2670.45	1765.18	3575.72	2.026	0.000
692057	SNORD12	small nucleolar RNA, C/D box 12	153.501	101.407	205.595	2.027	0.000
27068	PPA2	pyrophosphatase (inorganic) 2	2639.65	1742.16	3537.13	2.030	0.000
9975	NR1D2	nuclear receptor subfamily 1, group D, member 2	641.788	423.335	860.242	2.032	0.000
4285	MIPEP	mitochondrial intermediate peptidase	588.549	387.387	789.711	2.039	0.000
165055	CCDC138	coiled-coil domain containing 138	1099.30	723.278	1475.33	2.040	0.000
414241	FAM35BP	family with sequence similarity 35, member A pseudogene	2131.40	1400.7	2862.09	2.043	0.000
340554	ZC3H12B	zinc finger CCCH-type containing 12B	50.061	32.872	67.250	2.046	0.008
51187	RSL24D1	ribosomal L24 domain containing 1	12326.4	8086.64	16566.9	2.049	0.000
4698	NDUFA5	NADH dehydrogenase (ubiquinone) 1 alpha subcomplex, 5, 13kDa	1241.25	813.159	1669.34	2.053	0.000
8445	DYRK2	dual-specificity tyrosine-(Y)-phosphorylation regulated kinase 2	2404.27	1573.97	3234.57	2.055	0.000
5163	PDK1	pyruvate dehydrogenase kinase, isozyme 1	1812.33	1186.30	2438.36	2.055	0.000
283624	LINC00641	long intergenic non-protein coding RNA 641	325.172	212.704	437.640	2.058	0.000
287	ANK2	ankyrin 2, neuronal	41.125	26.889	55.361	2.059	0.009
23552	CDK20	cyclin-dependent kinase 20	89.008	58.196	119.821	2.059	0.001
81929	SEH1L	SEH1-like (S. cerevisiae)	2851.28	1850.98	3851.57	2.081	0.000
29078	NDUFAF4	NADH dehydrogenase (ubiquinone) complex I, assembly factor 4	268.801	174.305	363.296	2.084	0.000

1E+08	FPGT-TNNI3K	FPGT-TNNI3K readthrough	121.410	78.707	164.112	2.085	0.000
134728	IRAK1BP1	interleukin-1 receptor-associated kinase 1 binding protein 1	155.960	101.059	210.860	2.086	0.000
2649	NR6A1	nuclear receptor subfamily 6, group A, member 1	101.743	65.911	137.575	2.087	0.002
439965	FAM35DP	family with sequence similarity 35, member A pseudogene	2247.25	1455.14	3039.36	2.089	0.000
10560	SLC19A2	solute carrier family 19 (thiamine transporter), member 2	568.155	367.327	768.982	2.093	0.000
150709	ANKAR	ankyrin and armadillo repeat containing	41.483	26.808	56.158	2.095	0.007
9521	EEF1E1	eukaryotic translation elongation factor 1 epsilon 1	974.974	629.871	1320.08	2.096	0.000
1E+08	LOC100129461	uncharacterized LOC100129461	46.459	29.989	62.930	2.098	0.003
23742	NPAP1	nuclear pore associated protein 1	68.214	43.970	92.458	2.103	0.010
11222	MRPL3	mitochondrial ribosomal protein L3	7714.59	4966.17	10463.2	2.107	0.000
27340	UTP20	UTP20, small subunit (SSU) processome component, homolog (yeast)	1193.53	766.882	1620.17	2.113	0.000
80329	ULBP1	UL16 binding protein 1	33.592	21.545	45.639	2.118	0.008
79731	NARS2	asparaginyl-tRNA synthetase 2, mitochondrial (putative)	777.700	498.687	1056.71	2.119	0.000
85236	HIST1H2BK	histone cluster 1, H2bk	100.891	64.684	137.098	2.120	0.002
203197	C9orf91	chromosome 9 open reading frame 91	675.901	431.199	920.603	2.135	0.000
150094	SIK1	salt-inducible kinase 1	324.200	206.674	441.726	2.137	0.000
114899	C1QTNF3	C1q and tumor necrosis factor related protein 3	239.677	152.692	326.662	2.139	0.000
84842	HPDL	4-hydroxyphenylpyruvate dioxygenase-like	209.240	133.299	285.182	2.139	0.000
114614	MIR155HG	MIR155 host gene (non-protein coding)	532.994	339.395	726.594	2.141	0.000
10799	RPP40	ribonuclease P/MRP 40kDa subunit	445.720	283.603	607.837	2.143	0.000
1E+08	NA	NA	131.770	83.651	179.890	2.150	0.000
138199	C9orf41	chromosome 9 open reading frame 41	1038.7	659.342	1418.05	2.151	0.000
158135	TTLL11	tubulin tyrosine ligase-like family, member 11	39.399	25.005	53.793	2.151	0.006

3157	HMGCS1	3-hydroxy-3-methylglutaryl-CoA synthase 1 (soluble)	11383.7	7209.69	15557.8	2.158	0.000
79896	THNSL1	threonine synthase-like 1 (S. cerevisiae)	228.451	144.675	312.227	2.158	0.000
26806	SNORD44	small nucleolar RNA, C/D box 44	136.663	86.465	186.861	2.161	0.000
93587	TRMT10A	tRNA methyltransferase 10 homolog A (S. cerevisiae)	723.172	457.467	988.877	2.162	0.000
26996	GPR160	G protein-coupled receptor 160	1626.92	1028.81	2225.03	2.163	0.000
440	ASNS	asparagine synthetase (glutamine-hydrolyzing)	374.154	236.516	511.791	2.164	0.000
1E+08	NA	NA	33.943	21.430	46.457	2.168	0.006
7518	XRCC4	X-ray repair complementing defective repair in Chinese hamster cells 4	868.120	546.819	1189.42	2.175	0.000
5174	PDZK1	PDZ domain containing 1	57.432	36.174	78.690	2.175	0.002
91380	SNORD107	small nucleolar RNA, C/D box 107	46.629	29.322	63.936	2.180	0.002
692234	SNORD103A	small nucleolar RNA, C/D box 103A	60.182	37.809	82.554	2.183	0.001
692235	SNORD103B	small nucleolar RNA, C/D box 103B	60.182	37.809	82.554	2.183	0.001
79469	DLEU2L	deleted in lymphocytic leukemia 2-like	455.253	285.307	625.199	2.191	0.000
10274	STAG1	stromal antigen 1	946.130	589.598	1302.66	2.209	0.000
10622	POLR3G	polymerase (RNA) III (DNA directed) polypeptide G (32kD)	562.759	350.134	775.383	2.215	0.000
51175	TUBE1	tubulin, epsilon 1	450.466	279.329	621.602	2.225	0.000
79712	GTDC1	glycosyltransferase-like domain containing 1	284.158	176.050	392.266	2.228	0.000
728963	RPS15AP10	ribosomal protein S15a pseudogene 10	35.523	21.992	49.055	2.231	0.007
108	ADCY2	adenylate cyclase 2 (brain)	727.868	449.927	1005.81	2.235	0.000
112849	L3HYPDH	L-3-hydroxyproline dehydratase (trans-)	167.339	103.380	231.298	2.237	0.000
26770	SNORD79	small nucleolar RNA, C/D box 79	111.162	68.655	153.668	2.238	0.000
94015	TTYH2	tweety homolog 2 (Drosophila)	35.000	21.531	48.470	2.251	0.004
27165	GLS2	glutaminase 2 (liver, mitochondrial)	33.852	20.775	46.929	2.259	0.009
3899	AFF3	AF4/FMR2 family, member 3	3439.39	2108.32	4770.46	2.263	0.000

653643	GOLGA 6D	golgin A6 family, member D	32.747	20.072	45.422	2.263	0.005
388341	FAM211 A	family with sequence similarity 211, member A	42.352	25.904	58.799	2.270	0.003
56902	PNO1	partner of NOB1 homolog (S. cerevisiae)	1004.61	614.281	1394.94	2.271	0.000
230	ALDOC	aldolase C, fructose-bisphosphate	3099.87	1889.14	4310.60	2.282	0.000
64318	NOC3L	nucleolar complex associated 3 homolog (S. cerevisiae)	2228.05	1357.08	3099.02	2.284	0.000
54517	PUS7	pseudouridylate synthase 7 homolog (S. cerevisiae)	1029.92	623.433	1436.4	2.304	0.000
84546	SNORD 35B	small nucleolar RNA, C/D box 35B	27.668	16.707	38.629	2.312	0.008
10301	DLEU1	deleted in lymphocytic leukemia 1 (non-protein coding)	159.284	96.157	222.411	2.313	0.000
595100	SNORD 18C	small nucleolar RNA, C/D box 18C	52.582	31.724	73.439	2.315	0.001
7152	TOP1P2	topoisomerase (DNA) I pseudogene 2	122.143	73.519	170.767	2.323	0.000
9188	DDX21	DEAD (Asp-Glu-Ala-Asp) box helicase 21	15466.7	9287.88	21645.5	2.331	0.000
5080	PAX6	paired box 6	52.566	31.549	73.584	2.332	0.001
6936	GCFC2	GC-rich sequence DNA-binding factor 2	606.822	363.472	850.173	2.339	0.000
26802	SNORD 47	small nucleolar RNA, C/D box 47	537.969	322.001	753.937	2.341	0.000
51397	COMMD 10	COMM domain containing 10	291.991	174.647	409.335	2.344	0.000
400121	LINC00 547	long intergenic non-protein coding RNA 547	31.007	18.541	43.473	2.345	0.006
161436	EML5	echinoderm microtubule associated protein like 5	62.302	37.188	87.416	2.351	0.000
55889	GOLGA 6B	golgin A6 family, member B	31.623	18.831	44.414	2.359	0.003
63027	SLC22A 23	solute carrier family 22, member 23	51.223	30.440	72.006	2.366	0.001
4040	LRP6	low density lipoprotein receptor-related protein 6	81.694	48.352	115.036	2.379	0.000
131076	CCDC5 8	coiled-coil domain containing 58	2538.82	1496.47	3581.18	2.393	0.000
26049	FAM169 A	family with sequence similarity 169, member A	34.087	19.990	48.185	2.410	0.003
64172	OSGEP L1	O-sialoglycoprotein endopeptidase-like 1	364.511	213.403	515.619	2.416	0.000

1787	TRDMT1	tRNA aspartic acid methyltransferase 1	502.347	293.640	711.054	2.422	0.000
3112	HLA-DOB	major histocompatibility complex, class II, DO beta	28.411	16.607	40.215	2.422	0.006
283596	SNHG10	small nucleolar RNA host gene 10 (non-protein coding)	238.796	139.248	338.345	2.430	0.000
10785	WDR4	WD repeat domain 4	669.955	389.598	950.312	2.439	0.000
23251	KIAA1024	KIAA1024	79.253	46.069	112.437	2.441	0.000
677842	SNORA76	small nucleolar RNA, H/ACA box 76	41.052	23.759	58.344	2.456	0.001
200916	RPL22L1	ribosomal protein L22-like 1	372.474	215.517	529.430	2.457	0.000
388610	TRNP1	TMF1-regulated nuclear protein 1	55.254	31.806	78.702	2.474	0.000
441168	FAM26F	family with sequence similarity 26, member F	24.450	14.057	34.843	2.479	0.009
692201	SNORD86	small nucleolar RNA, C/D box 86	270.748	155.321	386.175	2.486	0.000
205	AK4	adenylate kinase 4	564.496	323.355	805.638	2.491	0.000
1E+08	LOC100130417	uncharacterized LOC100130417	45.959	26.190	65.729	2.510	0.003
2	A2M	alpha-2-macroglobulin	25.125	14.292	35.957	2.516	0.005
4609	MYC	v-myc myelocytomatosis viral oncogene homolog (avian)	5699.15	3231.63	8166.66	2.527	0.000
5071	PARK2	parkinson protein 2, E3 ubiquitin protein ligase (parkin)	139.868	79.285	200.451	2.528	0.000
9547	CXCL14	chemokine (C-X-C motif) ligand 14	34.504	19.480	49.528	2.543	0.001
144577	C12orf66	chromosome 12 open reading frame 66	229.226	129.410	329.043	2.543	0.000
692063	SNORA32	small nucleolar RNA, H/ACA box 32	50.302	28.208	72.397	2.567	0.000
692225	SNORD94	small nucleolar RNA, C/D box 94	150.135	83.964	216.307	2.576	0.000
9298	SNORD31	small nucleolar RNA, C/D box 31	42.449	23.708	61.190	2.581	0.001
8614	STC2	stanniocalcin 2	446.763	249.385	644.142	2.583	0.000
1E+08	NA	NA	67.857	37.838	97.876	2.587	0.000
1E+08	LOC100288974	BMS1 homolog, ribosome assembly protein (yeast) pseudogene	31.398	17.353	45.444	2.619	0.002
9303	SNORD25	small nucleolar RNA, C/D box 25	27.327	15.045	39.608	2.633	0.002
347686	SNORD64	small nucleolar RNA, C/D box 64	30.961	17.020	44.901	2.638	0.002

641455	POTEM	POTE ankyrin domain family, member M	83.877	45.606	122.149	2.678	0.000
23109	DDN	dendrin	48.985	26.514	71.456	2.695	0.000
653641	GOLGA6C	golgin A6 family, member C	29.436	15.927	42.945	2.696	0.002
6875	TAF4B	TAF4b RNA polymerase II, TATA box binding protein (TBP)-associated factor, 105kDa	728.306	393.380	1063.23	2.703	0.000
26805	SNORD45A	small nucleolar RNA, C/D box 45A	82.223	44.327	120.119	2.710	0.000
677805	SNORA18	small nucleolar RNA, H/ACA box 18	49.394	26.599	72.189	2.714	0.000
93986	FOXP2	forkhead box P2	938.972	499.863	1378.08	2.757	0.000
692072	SNORD5	small nucleolar RNA, C/D box 5	305.215	162.192	448.238	2.764	0.000
586	BCAT1	branched chain amino-acid transaminase 1, cytosolic	2687.73	1424.68	3950.78	2.773	0.000
407975	MIR17HG	miR-17-92 cluster host gene (non-protein coding)	610.929	315.614	906.245	2.871	0.000
1E+08	JARID2-AS1	JARID2 antisense RNA 1	23.099	11.888	34.309	2.886	0.005
1244	ABCC2	ATP-binding cassette, sub-family C (CFTR/MRP), member 2	34.055	17.432	50.678	2.907	0.000
645332	FAM86C2P	family with sequence similarity 86, member A pseudogene	68.313	34.937	101.688	2.911	0.000
1E+08	LINC00507	long intergenic non-protein coding RNA 507	52.157	26.635	77.678	2.916	0.002
1E+08	NA	NA	56.904	29.045	84.764	2.918	0.000
2200	FBN1	fibrillin 1	60.827	30.637	91.018	2.971	0.000
9300	SNORD28	small nucleolar RNA, C/D box 28	30.896	15.430	46.362	3.005	0.001
342096	GOLGA6A	golgin A6 family, member A	23.244	11.583	34.906	3.014	0.002
26769	SNORD81	small nucleolar RNA, C/D box 81	325.117	161.332	488.901	3.030	0.000
1E+08	NA	NA	227.225	112.619	341.830	3.035	0.000
677794	SNORA2B	small nucleolar RNA, H/ACA box 2B	17.537	8.684	26.391	3.039	0.004
407048	MIR92A1	microRNA 92a-1	26.716	13.144	40.287	3.065	0.001
54437	SEMA5B	sema domain, seven thrombospondin repeats (type 1 and type 1-like), transmembrane domain (TM) and short cytoplasmic domain, (semaphorin) 5B	24.265	11.925	36.605	3.070	0.001

26813	SNORD 36C	small nucleolar RNA, C/D box 36C	53.141	26.097	80.185	3.073	0.000
1E+08	MIR129 1	microRNA 1291	21.376	10.360	32.392	3.127	0.006
132203	SNTN	sentan, cilia apical structure protein	12.887	6.126	19.649	3.207	0.010
1E+08	SNORD 12B	small nucleolar RNA, C/D box 12B	33.116	15.528	50.704	3.265	0.000
3005	H1F0	H1 histone family, member 0	355.614	159.970	551.259	3.446	0.000
54898	ELOVL2	ELOVL fatty acid elongase 2	26.779	11.820	41.738	3.531	0.000
1E+08	DENND 5B-AS1	DENND5B antisense RNA 1	11.533	4.868	18.198	3.738	0.007
7881	KCNAB 1	potassium voltage-gated channel, shaker-related subfamily, beta member 1	14.676	6.104	23.249	3.809	0.002
753	LDLRA D4	low density lipoprotein receptor class A domain containing 4	183.545	75.059	292.031	3.891	0.000
406980	MIR19B 1	microRNA 19b-1	10.362	4.211	16.514	3.922	0.011
6414	SEPP1	selenoprotein P, plasma, 1	12.992	5.206	20.779	3.991	0.003
8350	HIST1H 3A	histone cluster 1, H3a	13.200	5.162	21.237	4.114	0.003
8336	HIST1H 2AM	histone cluster 1, H2am	54.971	20.923	89.020	4.255	0.010
723790	HIST2H 2AA4	histone cluster 2, H2aa4	376.195	138.145	614.245	4.446	0.006
8337	HIST2H 2AA3	histone cluster 2, H2aa3	376.195	138.145	614.245	4.446	0.006
1E+08	KCNQ5-IT1	KCNQ5 intronic transcript 1 (non-protein coding)	7.820	2.868	12.772	4.452	0.012
26768	RNU105 A	RNA, U105A small nucleolar	24.242	8.779	39.704	4.523	0.005
3006	HIST1H 1C	histone cluster 1, H1c	20.923	7.518	34.329	4.566	0.000
259293	TAS2R3 0	taste receptor, type 2, member 30	9.474	3.390	15.558	4.589	0.007
1E+08	NA	NA	9.512	3.390	15.635	4.612	0.006
8344	HIST1H 2BE	histone cluster 1, H2be	23.266	8.126	38.406	4.726	0.001
375316	RBM44	RNA binding motif protein 44	20.304	6.730	33.878	5.034	0.000
3698	ITIH2	inter-alpha-trypsin inhibitor heavy chain 2	22.824	7.413	38.235	5.158	0.000
554313	HIST2H 4B	histone cluster 2, H4b	26.201	8.410	43.993	5.231	0.000
8370	HIST2H 4A	histone cluster 2, H4a	26.201	8.410	43.993	5.231	0.000
692106	SNORD 65	small nucleolar RNA, C/D box 65	37.556	11.750	63.363	5.392	0.000

8347	HIST1H2BC	histone cluster 1, H2bc	11.113	3.472	18.753	5.401	0.008
8354	HIST1H3I	histone cluster 1, H3i	15.593	4.444	26.742	6.018	0.008
8357	HIST1H3H	histone cluster 1, H3h	7.232	1.961	12.503	6.376	0.007
57722	IGDCC4	immunoglobulin superfamily, DCC subclass, member 4	6.394	1.623	11.164	6.878	0.007
3012	HIST1H2AE	histone cluster 1, H2ae	30.796	7.793	53.798	6.903	0.001
8367	HIST1H4E	histone cluster 1, H4e	17.683	4.304	31.061	7.216	0.002
25805	BAMBI	BMP and activin membrane-bound inhibitor homolog (Xenopus laevis)	11.486	2.764	20.208	7.312	0.000
3008	HIST1H1E	histone cluster 1, H1e	12.376	2.969	21.782	7.336	0.004
317772	HIST2H2AB	histone cluster 2, H2ab	78.313	18.237	138.389	7.588	0.001
336	APOA2	apolipoprotein A-II	7.521	1.711	13.331	7.790	0.002
8332	HIST1H2AL	histone cluster 1, H2al	12.009	2.587	21.430	8.282	0.001
8341	HIST1H2BN	histone cluster 1, H2bn	8.933	1.761	16.106	9.146	0.003
8970	HIST1H2BJ	histone cluster 1, H2bj	12.418	2.431	22.405	9.215	0.000
8348	HIST1H2BO	histone cluster 1, H2bo	6.914	0.953	12.876	13.511	0.001
645752	LOC645752	golgin A6 family, member A pseudogene	5.340	0.714	9.965	13.950	0.002
335	APOA1	apolipoprotein A-I	7.199	0.953	13.444	14.108	0.001
8365	HIST1H4H	histone cluster 1, H4h	17.771	2.299	33.242	14.459	0.001
8339	HIST1H2BG	histone cluster 1, H2bg	19.291	2.438	36.143	14.822	0.001
1E+08	NA	NA	3.561	0.288	6.833	23.704	0.010
4907	NT5E	5'-nucleotidase, ecto (CD73)	4.414	0.332	8.496	25.564	0.003
1E+08	MIR1537	microRNA 1537	6.404	0.288	12.520	43.431	0.000
10202	DHRS2	dehydrogenase/reductase (SDR family) member 2	17.681	0.670	34.692	51.758	0.000
213	ALB	albumin	38.735	1.241	76.229	61.413	0.000
7018	TF	transferrin	13.178	0.288	26.067	90.421	0.000
23519	ANP32D	acidic (leucine-rich) nuclear phosphoprotein 32 family, member D	87.270	0.714	173.825	243.340	0.000
5950	RBP4	retinol binding protein 4, plasma	44.602	0.000	89.205	Inf	0.000

338	APOB	apolipoprotein B (including Ag(x) antigen)	38.002	0.000	76.004	Inf	0.000
174	AFP	alpha-fetoprotein	27.706	0.000	55.413	Inf	0.000
2719	GPC3	glypican 3	23.715	0.000	47.430	Inf	0.000
2266	FGG	fibrinogen gamma chain	15.417	0.000	30.835	Inf	0.000
197	AHSG	alpha-2-HS-glycoprotein	13.671	0.000	27.342	Inf	0.000
2243	FGA	fibrinogen alpha chain	12.360	0.000	24.721	Inf	0.000
3484	IGFBP1	insulin-like growth factor binding protein 1	7.259	0.000	14.519	Inf	0.000
401898	ZNF833P	zinc finger protein 833, pseudogene	3.789	0.000	7.577	Inf	0.002
259	AMBP	alpha-1-microglobulin/bikunin precursor	3.211	0.000	6.422	Inf	0.004
440077	ZNF705A	zinc finger protein 705A	2.769	0.000	5.538	Inf	0.009
3481	IGF2	insulin-like growth factor 2 (somatomedin A)	2.620	0.000	5.240	Inf	0.012
723961	INS-IGF2	INS-IGF2 readthrough	2.620	0.000	5.240	Inf	0.012

Table S1. Gene expression profile upon treatment with RAC1.